

# New analysis of the bounds from the electroweak precision tests on the 4-site model

Elena Accomando\* and Diego Becciolini†

*NExT Institute and School of Physics and Astronomy,  
University of Southampton, Highfield, Southampton SO17 1BJ, UK*

Luca Fedeli and Daniele Dominici‡

*Università degli Studi di Firenze, Dip. di Fisica e Astronomia, Firenze - Italy  
and Istituto Nazionale di Fisica Nucleare, Sezione di Firenze - Italy*

Stefania De Curtis§

*Istituto Nazionale di Fisica Nucleare, Sezione di Firenze - Italy*

(Dated: April 6, 2019)

We present a new complete analysis of the electroweak precision observables within the recently proposed 4-site Higgsless model, which is based on the  $SU(2)_L \times SU(2)_1 \times SU(2)_2 \times U(1)_Y$  gauge symmetry and predicts six extra gauge bosons,  $W_{1,2}^\pm$  and  $Z_{1,2}$ . Within the  $\varepsilon_i$  ( $i=1,2,3,b$ ) parametrization, we compute for the first time the EWPT bounds via a complete numerical algorithm going beyond commonly used approximations. Both  $\varepsilon_{1,3}$  impose strong constraints. Hence, it is mandatory to consider them jointly when extracting EWPT bounds and to fully take in to account the correlations among the electroweak precision measurements. The phenomenological consequence is that the extra gauge bosons must be heavier than 250 GeV. Their couplings to SM fermions, even if bounded, might be of the same order of magnitude than the SM ones. In contrast to other Higgsless models, the 4-site model is not fermiophobic. The new gauge bosons could thus be discovered in the favoured Drell-Yan channel already during the present run of the LHC experiment.

---

\*Electronic address: E.Accomando@soton.ac.uk

†Electronic address: diego.becciolini@soton.ac.uk

‡Electronic address: dominici@fi.infn.it, fedeli@fi.infn.it

§Electronic address: decurtis@fi.infn.it

## I. INTRODUCTION

In the past years a remarkable activity has been devoted to investigate electroweak models formulated in extra dimension space [1–11]. In most of these scenarios, the size and shape of the extra dimension(s) are responsible for solving the large hierarchy problem and they can also provide viable alternatives to the Higgs mechanism. For example, in models where the standard model (SM) gauge fields propagate in a fifth dimension, masses for the  $W^\pm$  and  $Z$  bosons can be generated via non-trivial boundary conditions [4, 6, 8–10]. Since the need for scalar doublets is eliminated in such scenarios, these models have been aptly dubbed *Higgsless models*. The result of allowing the SM gauge fields to propagate in the bulk, however, is towers of physical, massive vector gauge bosons (VGBs), the lightest of which are identified with the SM  $W^\pm$  and  $Z$  bosons. The heavier Kaluza-Klein (KK) modes, which have the  $SU(2) \times U(1)$  quantum numbers of the SM  $W^\pm$  and  $Z$ , play an important role in longitudinal VGB scattering. In the SM without a Higgs boson, the scattering amplitudes for these processes typically violate unitarity around  $\sim 1$  TeV [12]. The exchange of light Higgs bosons, however, cancels the unitarity-violating terms and ensures perturbativity of the theory up to high scales. In extra-dimensional Higgsless models, the exchange of the heavier KK gauge bosons plays the role of the Higgs boson and cancels the dominant unitarity-violating terms [4, 13–16]. As a result, the scale of unitarity violation can be pushed upward in the TeV range.

The main drawback of extra-dimensional models is that they are non-renormalizable and must be viewed as effective theories up to some cut-off scale  $\Lambda$  above which new physics must take over. An extremely efficient and convenient way of studying the phenomenology of five-dimensional effective theories in the context of four-dimensional gauge theories is that of deconstruction. In fact the discretization of the compact fifth dimension to a lattice generates the so-called deconstructed theories which are chiral Lagrangian with a number of replicas of the gauge group equal to the number of lattice sites [17–25]. Models have been proposed, assuming a  $SU(2)_L \times SU(2)_R \times U(1)_{B-L}$  gauge group in the 5D bulk, [4–7, 9–11, 26], in the framework suggested by the AdS/CFT correspondence, or also with a simpler gauge group  $SU(2)$  in the bulk [27–32]. Deconstructed models possess extended gauge symmetries which approximate the fifth dimension, but can be studied in the simplified language of coupled non-linear  $\sigma$ -models [33–35]. In fact, this method allows one to effectively separate the

perturbativity calculable contributions to low-energy observables from the strongly-coupled contributions due to physics above  $\Lambda$ . The former arise from the new weakly-coupled gauge states, while the latter can be parameterized by adding higher-dimensional operators [33–38].

The phenomenology of deconstructed Higgsless models has been well-studied [27–31, 37, 39, 40]. Recently, however, the simplest version of these types of models, which involves only three “sites”, has received much attention and been shown to be capable of approximating much of the interesting phenomenology associated with extra-dimensional models and more complicated deconstructed Higgsless models [10, 41–46]. The gauge structure of the 3-site model is identical to that of the so-called BESS (Breaking Electroweak Symmetry Strongly) which was first analyzed more than twenty years ago [47, 48]. Once electroweak symmetry breaking (EWSB) occurs in the 3-site model, the gauge sector consists of a massless photon, three relatively light massive VGBs which are identified with the SM  $W^\pm$  and  $Z$  gauge bosons, as well as three new heavy VGBs which we denote as  $W_1^\pm$  and  $Z_1$ . The exchange of these heavier states in longitudinal VGB scattering can delay unitarity violation up to higher scales (for discussions of unitarization through new vector states, see [27, 49–53]).

The drawback of all these models, as with technicolor theories, is to reconcile the presence of a relatively low KK-spectrum, necessary to delay the unitarity violation to TeV-energies, with the electroweak precision tests (EWPT) whose measurements can be expressed as functions of the  $\epsilon_1, \epsilon_2$  and  $\epsilon_3$  (or  $T, U, S$ ) parameters [54–57]. These parameters are defined in terms of the SM gauge boson self-energies,  $\Pi_{ij}^{\mu\nu}(q^2)$ , where  $(ij) = (WW), (ZZ), (\gamma\gamma)$  and  $(Z\gamma)$ , and  $q$  is the momentum carried by the external gauge bosons. More in detail, while  $\epsilon_1$  and  $\epsilon_2$  are protected by the custodial symmetry, shared by both the aforementioned classes of models, the  $\epsilon_3$  ( $S$ ) parameter constitutes the real obstacle to EWPT consistency. This problem can be solved by either delocalizing fermions along the fifth dimension [10, 42] or, equivalently in the deconstructed version of the model, by allowing for direct couplings between new vector bosons and SM fermions [45]. In the simplest version of this latter class of models, corresponding to just three lattice sites and gauge symmetry  $SU(2)_L \times SU(2) \times U(1)_Y$  (the BESS model), the requirement of vanishing of the  $\epsilon_3$  parameter implies that the new triplet of vector bosons is almost fermiophobic. As a consequence, the only production channels where the new gauge bosons can be searched for are those driven by boson-boson couplings. The Higgsless literature has been thus mostly focused on difficult multi-particle processes which require high luminosity to be detected, that is vector boson fusion and

associated production of new gauge bosons with SM ones [58–61].

The minimal 3-site model can be extended by inserting an additional lattice site. The newly obtained next-to-minimal (4-site) Higgsless model is based on the  $SU(2)_L \times SU(2)_1 \times SU(2)_2 \times U(1)_Y$  gauge symmetry. It predicts two neutral and four charged extra gauge bosons,  $Z_{1,2}$  and  $W_{1,2}^\pm$ , and satisfies the EWPT constraints without necessarily having fermiophobic resonances [53, 62, 63]. Within this framework, the more promising Drell-Yan processes become particularly relevant for the extra gauge boson search at the TEVATRON and the LHC.

In this paper, we present a new calculation of the EWPT bounds on the 4-site Higgsless model. There are two new ingredients compared to the existing results present in the literature. The first one concerns the computation of the 4-site Higgsless model contributions to the  $\varepsilon_i$  ( $i=1,2,3,b$ ) parameters, which summarize the electroweak precision measurements performed by LEP, SLD and TEVATRON experiments. These contributions are computed for the first time via a complete numerical algorithm, going beyond commonly used analytical approximations. The second ingredient addresses the minimum  $\chi^2$  test, used to extract bounds on the 4-site model. We improve previous simplified analysis, by taking into account the full correlation between the measurements of all four  $\varepsilon_i$  ( $i=1,2,3$ ) and  $\varepsilon_b$  [64] parameters. We moreover analyze the cutoff dependence of EWPT bounds, and discuss how well the 4-site Higgsless model can reproduce experimental results. We finally show the portion of the parameter space which survives the EWPT. Within that framework, we give a description of the main properties of the additional four charged and two neutral gauge bosons predicted by the 4-site Higgsless model.

The paper is structured as follows. In Sect.II, we review the next-to-minimal 4-site Higgsless model. In Sects.III-IV, we update the bounds from the EWPT and we derive the new allowed parameter space. Here, we define mass spectrum and gauge couplings of the extra  $Z_{1,2}$  and  $W_{1,2}^\pm$  vector bosons. In Sect.V, we compare the new exact results with those obtained via common approximations. Finally in Sect.VI, for completeness, we compute the new exact EWPT bounds on the minimal 3-site Higgsless model, and we compare quantitatively minimal and next-to-minimal Higgsless scenarios. Conclusions are given in Sect.VII. Appendix A contains, as a reference, the approximate calculations.

## II. REVIEW OF THE 4-SITE HIGGSLESS MODEL

The class of models we are interested in follows the idea of dimensional deconstruction [17–20] and was recently studied in [45]. The so-classified theories can also be seen as a generalization of the BESS model [47, 48, 65] to an arbitrary number of new triplets of gauge bosons. In their general formulation [27–31], they are based on the  $SU(2)_L \otimes SU(2)^K \otimes U(1)_Y$  gauge symmetry, and contain  $K + 1$  non-linear  $\sigma$ -model scalar fields which trigger the spontaneous symmetry breaking.

The 4-site Higgsless model, described in Refs.[53, 62, 63], is defined by taking  $K=2$  and requiring the Left-Right (LR) symmetry in the gauge sector. In the unitary gauge, it predicts two new triplets of gauge bosons which acquire mass through the same symmetry breaking mechanism which gives mass to the SM gauge bosons. By calling  $\tilde{W}_{i\mu} = \tilde{W}_{i\mu}^a \tau^a / 2$  and  $g_i$  the gauge fields and couplings associated to the extra  $SU(2)_i$ ,  $i = 1, 2$ ;  $\tilde{W}_\mu = \tilde{W}_\mu^a \tau^a / 2$ ,  $\tilde{Y}_\mu = \tilde{\mathcal{Y}}_\mu \tau^3 / 2$  and  $\tilde{g}$ ,  $\tilde{g}'$  the gauge fields and couplings associated to  $SU(2)_L$  and  $U(1)_Y$  respectively, the charged gauge boson mass Lagrangian is given by:

$$\mathcal{L}_{mass}^C = \tilde{\mathcal{C}}_\mu^- \mathcal{M}_c^2 \tilde{\mathcal{C}}^{\mu+} \quad (1)$$

with  $\tilde{\mathcal{C}}^- = (\tilde{W}^-, \tilde{W}_1^-, \tilde{W}_2^-)$ ,  $\tilde{\mathcal{C}}^+ = (\tilde{\mathcal{C}}^-)^\dagger$ , and

$$\mathcal{M}_c^2 = \begin{pmatrix} \frac{\tilde{g}^2}{g_1^2} M_1^2 & -\frac{\tilde{g}}{g_1} M_1^2 & 0 \\ -\frac{\tilde{g}}{g_1} M_1^2 & \frac{1}{2}(M_1^2 + M_2^2) & \frac{1}{2}(M_1^2 - M_2^2) \\ 0 & \frac{1}{2}(M_1^2 - M_2^2) & \frac{1}{2}(M_1^2 + M_2^2) \end{pmatrix} \quad (2)$$

where  $M_{1,2}$  are the bare masses of the six additional gauge bosons,  $W_{1,2}^\pm$ ,  $Z_{1,2}$  and we had taken  $g_1 = g_2$  in virtue of the LR symmetry imposed in the gauge sector.

Similarly, the mass Lagrangian of the neutral gauge sector is:

$$\mathcal{L}_{mass}^N = \frac{1}{2} \tilde{N}_\mu^T \mathcal{M}_n^2 \tilde{N}^\mu \quad (3)$$

with  $\tilde{N}^T = (\tilde{W}^3, \tilde{W}_1^3, \tilde{W}_2^3, \tilde{\mathcal{Y}})$  and

$$\mathcal{M}_n^2 = \begin{pmatrix} \frac{\tilde{g}^2}{g_1^2} M_1^2 & -\frac{\tilde{g}}{g_1} M_1^2 & 0 & 0 \\ -\frac{\tilde{g}}{g_1} M_1^2 & \frac{1}{2}(M_1^2 + M_2^2) & \frac{1}{2}(M_1^2 - M_2^2) & 0 \\ 0 & \frac{1}{2}(M_1^2 - M_2^2) & \frac{1}{2}(M_1^2 + M_2^2) & -\frac{\tilde{g}'}{g_1} M_1^2 \\ 0 & 0 & -\frac{\tilde{g}'}{g_1} M_1^2 & \frac{\tilde{g}'^2}{g_1^2} M_1^2 \end{pmatrix} \quad (4)$$

Direct couplings of the new gauge bosons to SM fermions can be included in a way that preserves the symmetry of the model. The fermion Lagrangian is given by:

$$\begin{aligned}
\mathcal{L}_{fermions} = & \bar{\psi}_L i\gamma^\mu \partial_\mu \psi_L + \bar{\psi}_R i\gamma^\mu \partial_\mu \psi_R \\
& - \frac{1}{1+b_1+b_2} \bar{\psi}_L \gamma^\mu \tilde{g} \tilde{W}_\mu \psi_L \\
& - \sum_{i=1}^2 \frac{b_i}{1+b_1+b_2} \bar{\psi}_L \gamma^\mu g_i \tilde{W}_{i\mu} \psi_L \\
& - \bar{\psi}_R \gamma^\mu (\tilde{g}' \tilde{Y}_\mu + \frac{1}{2} \tilde{g}' (B-L) \tilde{\mathcal{Y}}_\mu) \psi_R - \bar{\psi}_L \gamma^\mu \frac{1}{2} \tilde{g}' (B-L) \tilde{\mathcal{Y}}_\mu \psi_L.
\end{aligned} \tag{5}$$

In the above formula,  $b_{1,2}$  are two arbitrary dimensionless parameters, which we assume to be the same for quarks and fermions of each generation, and  $\psi_{L(R)}$  denotes the standard quarks and leptons. Direct couplings of the new gauge bosons to SM right-handed fermions could also be introduced. They are however strongly constrained by data from non-leptonic K-decays and  $b \rightarrow s\gamma$  processes [66] to be of order of  $10^{-3}$  [67]. For this reason, we neglect them.

The 4-site Higgsless model contains seven parameters a priori:  $\tilde{g}, \tilde{g}', g_1, M_1, M_2, b_1, b_2$ . However, their number can be reduced to four, by fixing the gauge couplings  $\tilde{g}, \tilde{g}', g_1$  in terms of the three SM input parameters  $e, G_F, M_Z$  which denote electric charge, Fermi constant and Z-boson mass, respectively. As a result, our parameter space is defined by four free parameters:  $M_{1,2}$  which represent the bare masses of the lighter ( $W_1^\pm, Z_1$ ) and heavier ( $W_2^\pm, Z_2$ ) gauge boson triplets, and  $b_{1,2}$  which are their bare direct couplings to SM fermions. In the following, we will give our results also in terms of  $z = M_1/M_2$ , the ratio of the bare masses.

### A. Free parameters versus physical observables

Before starting the new analysis of the EWPT bounds on the 4-site Higgsless model, it is useful to understand how the free parameters of the model are connected to the physical quantities. We focus here on the gauge sector (the fermionic one will be discussed later in Sect.IV) and we analyze the relation between mass eigenvalues and bare masses,  $M_{1,2}$ . The results are displayed in Fig. 1. In the left plot, we show the ratio between physical and bare masses,  $M_{Vi}/M_i$  ( $V = W, Z$  and  $i=1,2$ ), as a function of  $z = M_1/M_2$  for a given repre-

sentative value  $M_1=0.4$  TeV. Let us notice that the mass eigenvalues acquire a dependence on the direct couplings between extra gauge bosons and ordinary matter,  $b_{1,2}$ , via the  $G_F$  constraint. This dependence is however quite mild. Thus, at fixed  $M_1$ , everything is driven by the  $z$  parameter and we can safely fix  $b_{1,2} = 0$ . From the left plot in Fig. 1, one can see that the corrections to the bare mass parameters are positive. More in detail, they do not exceed  $\mathcal{O}(5\%)$  for low-intermediate values of  $z$ , while they sensibly increase up to  $\mathcal{O}(30\%)$  for high  $z$  values. This behavior characterizes the low-intermediate mass spectrum, which the chosen  $M_1=0.4$  TeV value in Fig. 1 is an example of. The situation changes drastically, and gets more stable, if one moves to larger mass scales. For  $M_1 \geq 1$  TeV indeed the corrections to the bare masses never exceed  $\mathcal{O}(5\%)$  over the full  $z$  range. We can observe a similar behavior in the ratio between the masses of lighter and heavier extra gauge bosons. In the right plot of Fig. 1, we compare  $z = M_1/M_2$  with the corresponding ratios between the mass eigenvalues of charged and neutral extra gauge bosons. We fix, as before,  $M_1=0.4$  TeV and

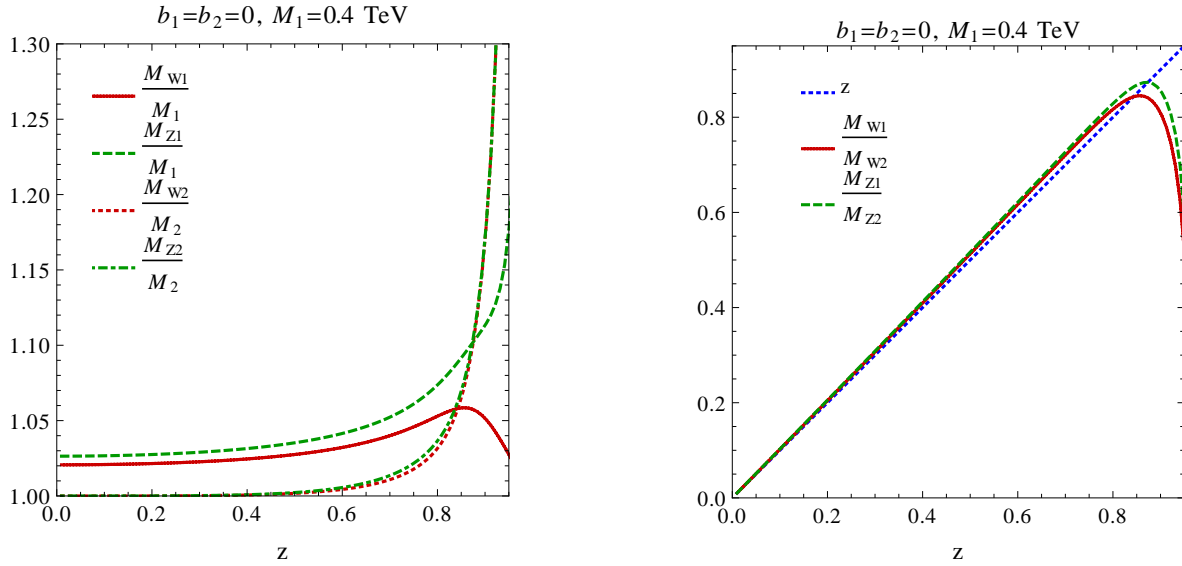


FIG. 1: Left: Ratios  $M_{W_i}/M_i$ ,  $M_{Z_i}/M_i$  ( $i = 1, 2$ ) as a function of  $z = M_1/M_2$  at fixed  $M_1=0.4$  TeV. Right: Ratios  $M_{W1}/M_{W2}$ ,  $M_{Z1}/M_{Z2}$ , and  $z = M_1/M_2$  as a function of  $z$  at fixed  $M_1=0.4$  TeV. We fix  $b_{1,2} = 0$ .

plot the three different ratios  $z$ ,  $M_{W1}/M_{W2}$  and  $M_{Z1}/M_{Z2}$  versus  $z$ . Once again, the bare parameter  $z = M_1/M_2$  appears to be a good approximation of the ratio between  $M_{W1,Z1}$  and  $M_{W2,Z2}$  except for low masses  $M_1 \leq 1$  TeV and high  $z$  values where it can overestimate the

physical ratios up to about 40%. In this latter region in fact the corrections to  $M_2$  are much stronger than those to  $M_1$ , as shown in the left plot, giving rise to a sharp decrease in the  $M_{W1}/M_{W2}$  and  $M_{Z1}/M_{Z2}$  ratios compared to the bare  $z$  value. Thus summarizing, in the low-intermediate  $z$  region, the bare parameters give an excellent description of the physical quantities, accurate at percent level for low masses, and at permil level for  $\mathcal{O}(\text{TeV})$  masses. In the high  $z$  region instead, the bare parameters give a good estimate of the physical masses only for  $M_1 \geq 1$  TeV, while the low edge of the spectrum is poorly reproduced.

The above mentioned physical masses and couplings of the extra gauge bosons to ordinary matter are obtained via a complete numerical algorithm in terms of the four free parameters of the model:  $M_1$ ,  $z$ ,  $b_1$ ,  $b_2$ . This represents a novelty compared to previous publications [53, 62, 63]. The outcome is the ability to reliably and accurately describe the full parameter space of the 4-site Higgsless model even in regions of low mass and high  $z$  where previously used approximations would fail, as we will discuss in detail in Sect.V.

### III. BOUNDS FROM EWPT: UPDATE OF THE $\varepsilon_{1,2,3,b}$ ANALYSIS

Universal electroweak radiative corrections to the precision observables measured by LEP, SLD and TEVATRON experiments can be efficiently quantified in terms of three parameters:  $\varepsilon_1$ ,  $\varepsilon_2$ , and  $\varepsilon_3$  (or S, T, and U) [54–57]. A fourth parameter,  $\varepsilon_b$ , can be added to describe non universal effects associated to the bottom quark sector [64]. Besides the SM contributions, also potential heavy new physics may affect the low-energy electroweak precision data through these four parameters. For that reason, the  $\varepsilon_i$  ( $i=1,2,3,b$ ) are a powerful method to constrain theories beyond the SM. We use this parametrization to derive bounds on the 3-site (or BESS) and 4-site Higgsless models. Measurements by the LEP2 experiment can be summarized in four additional parameters  $V, X, Y, W$  [68]. However, the 3-site and 4-site model contributions to these observables are strongly suppressed. We thus neglect them, and focus only on the  $\varepsilon_i$  ( $i=1,2,3,b$ ) parameters.

In the literature on Higgsless models, major attention has been devoted to the  $\varepsilon_3$  (or S) parameter. The computations have been performed mainly at tree level, by making use of different approximations. The common feature of these approximate results is that they all rely on a series expansion in the ratio  $e/g_1$ , where  $e$  is the electric charge and  $g_1$  the extra gauge group coupling constant, and in the model parameters which measure



the amount of fermion delocalization in the five dimensional theory interpretation (in the deconstructed version they are represented by the  $b_i$  parameters). In this approximation, the  $\varepsilon_{1,2}$  parameters vanish at tree level owing to the custodial symmetry, at least at the first order in the fermion delocalization parameter expansion. This is the reason why most of the physics community has focused on  $\varepsilon_3$ . In addition to the discussed approximate tree level results, in the recent years preliminary calculations of one-loop corrections have been performed. More in detail, the one-loop chiral logarithmic corrections to the  $\varepsilon_{1,3}$  (or T and S) parameters have been evaluated for the 3-site and 4-site models [69–72]. At the present status of the  $\varepsilon_i$  calculation, the one-loop contribution to the  $\varepsilon_1$  parameter is of course dominant.

In this paper, we aim to fill the gap between approximate tree level results and attempts of improved precision at one-loop. We concentrate on the tree level calculation, going beyond the popular approximations summarized above. We thus compute the four  $\varepsilon_i$  ( $i=1,2,3,b$ ) exactly, keeping their full dependence on the model parameters, via a numerical algorithm. In order to understand quantitatively the difference between exact and approximate results, and maintain a link with the previous literature, in Sec.V we will compare our exact numerical calculation with the approximate expansion up to the second order in the  $e/g_1$  parameter, keeping the  $b_i$  direct coupling content exact. The physical motivation to go beyond the first order perturbative expansion of the  $\varepsilon_i$  ( $i=1,2,3,b$ ) in the model parameters is three-fold. The first reason is to give a complete description of the parameter space. As the bare mass parameter  $M_1$  is roughly proportional to the gauge coupling  $g_1$ , and strictly linked to the physical masses  $M_{W1,Z1}$ , in order to reach the low edge of the spectrum one has to deal with small  $g_1$  values where the expansion in  $e/g_1$  is not reliable anymore. In addition, the contributions to the  $\varepsilon_i$  coming from the direct couplings between SM fermions and new vector bosons,  $b_{1,2}$ , either induced by the presence of new heavy fermions or by the fermion delocalization in the bulk when considering theories in five dimensions, can undergo delicate cancelations. While in the 3-site model there is only one bare direct coupling, and fine-tuned to keep the fermion couplings of the new gauge bosons very small in order to accommodate EWPT (almost fermiophobic scenario), in the 4-site extension of Higgsless models there are two bare direct couplings, thus some interplay between them, allowing for larger couplings within the bounds. In this latter case, subtle cancelations take place and the perturbative expansion up to the first order in the fermion-boson direct couplings (or

fermion delocalization parameter) is not good anymore. Finally,  $\varepsilon_{1,2,3}$  receive logarithmic loop corrections from SM particles which increase with energy. Within the SM, such a bad high energy behavior is cutoff by the mass of a light Higgs. But, obviously, in Higgsless models these contributions become extremely important when approaching  $O(\text{TeV})$  energy scales. It is thus necessary to compute precisely not only  $\varepsilon_3$  but also  $\varepsilon_{1,2}$  in order to see whether the new physics, alternative to the light elementary Higgs, can balance the bad SM logarithmic growth with energy. For all these reasons, in order to derive realistic and reliable bounds on Higgsless models it is mandatory to exactly compute all  $\varepsilon_i$  ( $i=1,2,3,b$ ) parameters, and perform a combined fit to the experimental results taking into account their full correlation.

#### A. Computing $\varepsilon_1, \varepsilon_2, \varepsilon_3$ , and $\varepsilon_b$ in the 4-Site Higgsless model.

The three electroweak  $\varepsilon_i$  ( $i=1,2,3$ ) parameters, summarizing the universal electroweak corrections to the precision observables measured by LEP, SLD and TEVATRON, can be obtained from  $\Delta r_W$ ,  $\Delta\rho$  and  $\Delta k$  [57, 64]:

$$\begin{aligned}\epsilon_1 &= \Delta\rho \\ \epsilon_2 &= c_\theta^2 \Delta\rho + \frac{s_\theta^2}{c_{2\theta}} \Delta r_W - 2s_\theta^2 \Delta k \\ \epsilon_3 &= c_\theta^2 \Delta\rho + c_{2\theta} \Delta k\end{aligned}\tag{6}$$

with the Weinberg angle defined by

$$s_\theta^2 c_\theta^2 = \frac{\sqrt{2}e^2}{8M_Z^2 G_F}.\tag{7}$$

In this scheme, the physical inputs are chosen to be the electric charge, the Fermi constant and the  $Z$ -boson mass:

$$\sqrt{4\pi\alpha} = 0.3123\tag{8}$$

$$G_F = 1.16639 \times 10^{-5} \text{ GeV}^{-2}\tag{9}$$

$$M_Z = 91.1876 \text{ GeV}\tag{10}$$

The Weinberg angle is thus uniquely determined. The fourth  $\varepsilon_b$  parameter, describing instead non-universal effects in the bottom quark sector, is related to the corrections to the

SM  $Z$ -boson coupling to left-handed  $b$ -quarks,  $\delta g_{Lb}$ , as follows:

$$\varepsilon_b = -2\delta g_{Lb}. \quad (11)$$

Within the 4-site Higgsless model, the  $\varepsilon_b$  parameter is zero owing to family universality in the fermionic sector. It receives however a contribution from SM radiative corrections, and it is experimentally correlated to the other three  $\varepsilon_i$  ( $i=1,2,3$ ) parameters. For this reason, we analyze its effect. In principle a non universality of direct couplings could be considered for the  $(t, b)$  sector to describe a special role of this doublet due to its possible compositeness [5, 11, 73–78]. In this paper we don't consider such an alternative.

In order to compute the new physics contributions to the  $\varepsilon_i$  ( $i=1,2,3$ ) parameters, we follow the procedure of diagonalizing the charged and neutral mass matrices. We thus derive the mass eigenstates of the gauge sector, and recast the Lagrangian in terms of those eigenvectors. Once the Lagrangian given in Eq. (5) has been re-expressed in terms of charged and neutral gauge boson mass eigenstates, the two  $\Delta\rho$  and  $\Delta k$  parameters can be extracted from the neutral current couplings to the SM  $Z$ -boson:

$$\mathcal{L}^{neutral}(Z) = -\frac{e}{s_\theta c_\theta} \left(1 + \frac{\Delta\rho}{2}\right) Z_\mu \bar{\psi} [\gamma^\mu g_V + \gamma^\mu \gamma_5 g_A] \psi \quad (12)$$

with

$$g_V = \frac{\mathbf{T}^3}{2} - s_{\theta_{eff}}^2 \mathbf{Q}, \quad g_A = -\frac{\mathbf{T}^3}{2}, \quad s_{\theta_{eff}}^2 = (1 + \Delta k) s_\theta^2. \quad (13)$$

The  $\Delta r_W$  parameter is instead given by:

$$\frac{M_W^2}{M_Z^2} = c_\theta^2 \left[ 1 - \frac{s_\theta^2}{c_{2\theta}} \Delta r_W \right] \quad (14)$$

where  $M_W$  and  $M_Z$  are the SM  $W^\pm$  and  $Z$  boson masses.

The tree level contribution of the 4-site Higgsless model to the  $\varepsilon_i$  ( $i=1,2,3$ ) parameters has been computed exactly, via a complete numerical calculation. This represents a novelty. In the literature, in fact, these tree level new physics effects are evaluated via an analytical truncated multiple expansion in the extra gauge coupling,  $e/g_1$ , and the direct couplings of the extra gauge bosons with SM fermions (or delocalization parameters), that is  $b_{1,2}$  in our notation. The exact result we present in this paper allows one to span the full parameter space of the model, reliably computing also regions characterized by small  $g_1$  (or  $M_1$ ) values, and sizable  $b_{1,2}$  couplings where the common approximated expansion would fail. For sake of comparison, in Appendix A we derive the  $\varepsilon_i$  parameters via an analytical expansion up

to the order  $\mathcal{O}(e^2/g_1^2)$ , keeping the full  $b_{1,2}$  content. In Sec.V, we discuss the goodness of this approximation, and define its validity domain by comparing it to the exact numerical solution.

### B. Fit to the ElectroWeak Precision Tests

By making use of the electroweak precision observables measured by LEP, SLD and TEVATRON experiments, one can determine the  $\varepsilon_i$  ( $i=1,2,3,b$ ) parameters as [79]

$$\begin{aligned} \varepsilon_1^{exp} &= +(5.4 \pm 1.0) \cdot 10^{-3} \\ \varepsilon_2^{exp} &= -(8.9 \pm 1.2) \cdot 10^{-3} \\ \varepsilon_3^{exp} &= +(5.34 \pm 0.94) \cdot 10^{-3} \\ \varepsilon_b^{exp} &= -(5.0 \pm 1.6) \cdot 10^{-3} \end{aligned} \quad \rho = \begin{pmatrix} 1 & 0.60 & 0.86 & 0.00 \\ 0.60 & 1 & 0.40 & -0.01 \\ 0.86 & 0.40 & 1 & 0.02 \\ 0.00 & -0.01 & 0.02 & 1 \end{pmatrix} \quad (15)$$

where  $\rho$  is the correlation matrix. In order to perform a complete EWPT analysis and pose constraints on the parameters of the 4-site Higgsless model, we need to include also the SM universal electroweak radiative corrections to the four  $\varepsilon_i$  parameters. We make use of the following expressions, obtained with the code TopaZ0 to compute the radiative corrections with  $m_t^{pole} = 172.7$  GeV [80]:

$$\varepsilon_1^{rad} = (+5.6 - 0.86 \ln \frac{M_H}{M_Z}) 10^{-3} \quad (16)$$

$$\varepsilon_2^{rad} = (-7.09 + 0.16 \ln \frac{M_H}{M_Z}) 10^{-3} \quad (17)$$

$$\varepsilon_3^{rad} = (+5.25 + 0.54 \ln \frac{M_H}{M_Z}) 10^{-3} \quad (18)$$

$$\varepsilon_b^{rad} = -6.43 \cdot 10^{-3}. \quad (19)$$

These equations represent an effective and sufficiently accurate numerical approximation of the pure SM contribution. The Higgs mass,  $M_H$ , should be interpreted in our model as an ultraviolet cutoff of the SM loops provided by the model itself. These terms correspond to UV logarithms in the low energy Higgsless theory. We will take  $M_H = 1, 3$  TeV. The first case corresponds to the extrapolated SM predictions in presence of a scalar bound state which saturates the Lee-Quigg-Thacker bound [12]. The second corresponds to the case with no bound state and  $M_H$  is interpreted as the cutoff of the theory. For comparison with the SM fit, we will consider also a case with  $M_H = 300$  GeV.

We are now ready to extract bounds on the free parameters of the 4-site Higgsless model,  $M_{1,2}$  and  $b_{1,2}$ , by performing a minimum  $\chi^2$  test. The  $\chi^2$  function is defined as:

$$\chi^2 = \sum_{i,j} (\varepsilon_i - \varepsilon_i^{rad} - \varepsilon_i^{exp})(\sigma^2)_{ij}^{-1}(\varepsilon_j - \varepsilon_j^{rad} - \varepsilon_j^{exp}), \quad \text{where} \quad (\sigma^2)_{ij} = \sigma_i \rho_{ij} \sigma_j .$$

In the above equation,  $\sigma_i$  is the standard deviation and  $\rho_{ij}$  the correlation matrix of Eq. (15). The global minimum  $\chi^2$ , obtained by minimizing with respect to the four free parameters  $M_{1,2}$  and  $b_{1,2}$ , is denoted by  $\chi_{min}^2$ . In order to define our allowed parameter space, we keep only points which satisfy the following condition:

$$\Delta\chi^2 = \chi^2 - \chi_{min}^2 \leq 9.49(13.28) \quad (20)$$

where the value 9.49(13.28) corresponds to a 95(99)% Confidence Level (CL) for a  $\chi^2$  with four degrees of freedom (dof). To better visualize the allowed regions of the parameter space, we will project the four-dimensional space into different planes. In this way, we will display the 95(99)% CL EWPT bounds on different selected pairs of free parameters.

But, before doing that, let us first discuss the statistical concept of goodness-of-fit, which describes how well a theoretical model fits a set of measurements. Qualitative arguments suggest that it can be summarized by the condition  $\chi_{min}^2 \simeq \text{dof}$ . In Fig. 2, we compare the goodness-of-fit of the 4-site Higgsless model to electroweak precision data expressed in terms of the  $\varepsilon_i$  parameters (right plot) with the analogous goodness-of-fit of the Standard Model (left plot). In the right plot of Fig. 2, we fix  $z = M_1/M_2 = 0.8$ , and show how the  $\chi^2$ -function varies with  $M_1$  once minimizing over the two remaining  $b_{1,2}$  free parameters. The solid lines correspond to the correlated  $\varepsilon_{1,2,3}$  analysis. The dashed curves include also  $\varepsilon_b$ . Fig. 2 clearly shows that  $\varepsilon_b$  does not give a relevant contribution to the 4-site Higgsless model test, and justifies our choice to neglect it from now on, also, the  $\varepsilon_b$  measurement is poorly correlated to the others (see Eq. (15)). From top to bottom, the three solid lines give the  $\chi^2$  function for three different values of the  $M_H$  parameter in Eq. (19):  $M_H = 3, 1, 0.3$  TeV respectively. Independently on the value of  $M_H$ , the  $\chi^2$  function is almost flat in the  $M_{1,2}$  mass parameters, except at very low bare masses where it rapidly increases. All  $z$  values share the same feature. Thus, there is not a clear minimum  $\chi^2$  in the  $M_{1,2}$  masses. The second information displayed in Fig. 2 is the strong dependence of the  $\chi^2$  function on the  $M_H$  parameter. The  $\chi^2$  increase with  $M_H$  reflects the well known conflict between cut-off scale and new physics content. The  $\chi^2$  values obtained within the 4-site Higgsless model can be compared with the SM  $\chi^2$  for

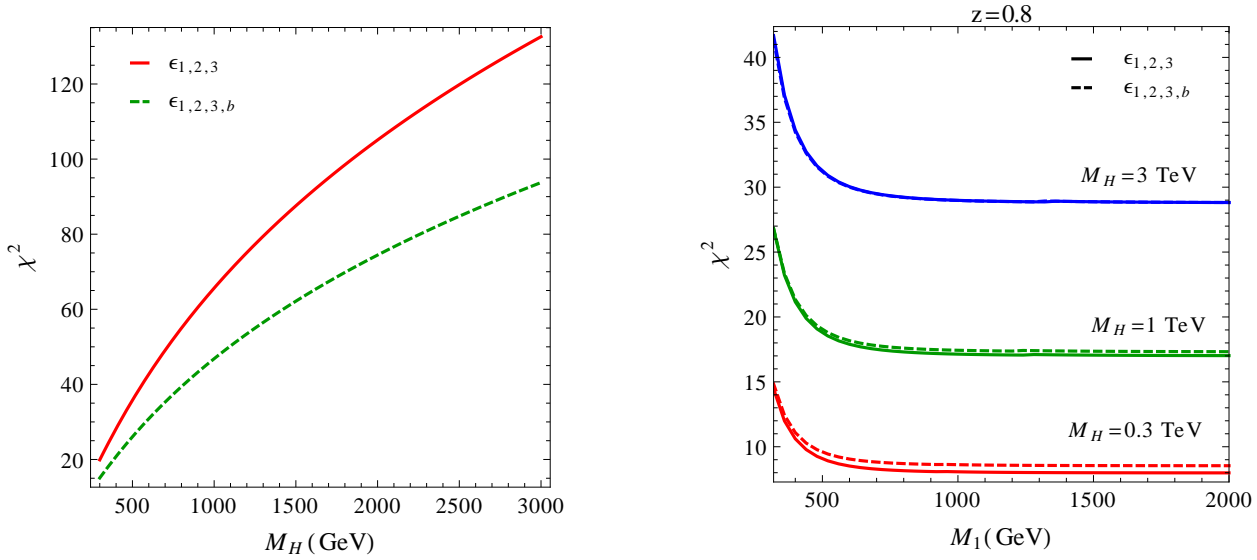


FIG. 2: Left:  $\chi^2$ -function versus the Higgs mass,  $M_H$ , within the SM. The solid line comes from the correlated  $\epsilon_{1,2,3}$  analysis, the dashed one includes also the correlated  $\epsilon_b$  parameter. Right:  $\chi^2$ -function versus the bare mass  $M_1$ , within the 4-site Higgsless model at fixed  $z = M_1/M_2 = 0.8$ , after minimizing over the two remaining free parameters,  $b_{1,2}$ . The solid line comes from the correlated  $\epsilon_{1,2,3}$  analysis, the dashed one includes also the correlated  $\epsilon_b$  parameter. From bottom to top, the three sets of curves correspond to the following three values of the  $M_H$  parameter:  $M_H=0.3, 1, 3$  TeV.

the same  $M_H$  values. The SM  $\chi^2$  function versus  $M_H$  is shown in the left plot of Fig. 2. In this way, the balance between  $M_H$  dependent terms and new physics contributions to the  $\epsilon_i$  parameters is evident. The dramatic growth of the SM  $\chi^2$  function with increasing the  $M_H$  parameter is largely compensated by the new physics content predicted by the 4-site Higgsless model. This shows that, despite the fact that Higgsless models are characterized by large minimum  $\chi^2$  values thus failing the goodness-of-fit thumb rule  $\chi^2_{min}/\text{dof} \leq 1$ , they succeed in curing the non-linear  $\sigma$ -model and represent a viable alternative to the SM with a few hundred Higgs mass ( $\chi^2_{SM}(M_H = 0.3 \text{ TeV}) \sim \chi^2_{min}(M_H = 1 \text{ TeV})$ ).

## IV. MASS SPECTRUM AND COUPLINGS OF THE EXTRA $W_{1,2}^\pm$ AND $Z_{1,2}$ GAUGE BOSONS

In this section, we derive the EWPT bounds on mass spectrum and couplings of the extra  $W_{1,2}^\pm$  and  $Z_{1,2}$  gauge bosons to ordinary matter. The aim is giving a complete definition of the physical properties of the new vector resonances predicted by the 4-site Higgsless model, needed for any phenomenological analysis.

### A. Mass spectrum

A first information to be derived concerns the possible existence of a minimum allowed mass for the six extra resonances,  $W_{1,2}^\pm$  and  $Z_{1,2}$ , predicted by the 4-site Higgsless model. In order to derive that, in the left plot of Fig. 3 we show  $\Delta\chi^2 = \chi^2(z, M_1) - \chi_{min}^2$  as a function of  $M_1$  for four representative  $z$  values:  $z=0.1, 0.4, 0.8$  and  $0.95$ . We fix  $M_H=3$  TeV. The function  $\chi^2(z, M_1)$  is computed by minimizing over the two remaining  $b_{1,2}$  parameters, while  $\chi_{min}^2$  denotes the minimum  $\chi^2$  value over all four free parameters of the model. We use the correlated  $\epsilon_{1,2,3}$  analysis of Eq. (15). The intersection of the above mentioned four curves with the solid horizontal lines gives the 95% and 99% CL lower bound on the bare mass of the lighter extra gauge boson,  $M_1$ , according to Eq. (20). We now need to translate such a value into the minimum allowed physical mass for  $W_{1,2}^\pm$  and  $Z_{1,2}$  gauge bosons, taking into account the corrections to the bare mass parameter discussed in the previous section. In the right plot of Fig. 3, we display the 95% CL contour in the  $(z, M_{W1})$  plane for the two reference values of the  $M_H$  parameter:  $M_H=1$  and 3 TeV. As one can see, the increase in  $M_H$  gives a minor effect, shifting the minimum allowed mass by roughly 50 GeV, independently on  $z$ .

### B. $W_{1,2}^\pm$ and $Z_{1,2}$ gauge boson couplings to SM fermions

In this section, we extract the EWPT bounds on the physical couplings of the extra gauge bosons with ordinary matter. To this aim, we start deriving the EWPT constraints on the two free parameters of the 4-site Higgsless model,  $b_{1,2}$ , which represent the bare direct boson-fermion gauge couplings. We project the  $\chi^2$  condition given in Eq. (20) on the  $b_1, b_2$  plane at fixed values of the two remaining parameters:  $z=0.8$  and  $M_1=0.8$  TeV (i.e.  $M_2=1$  TeV). The

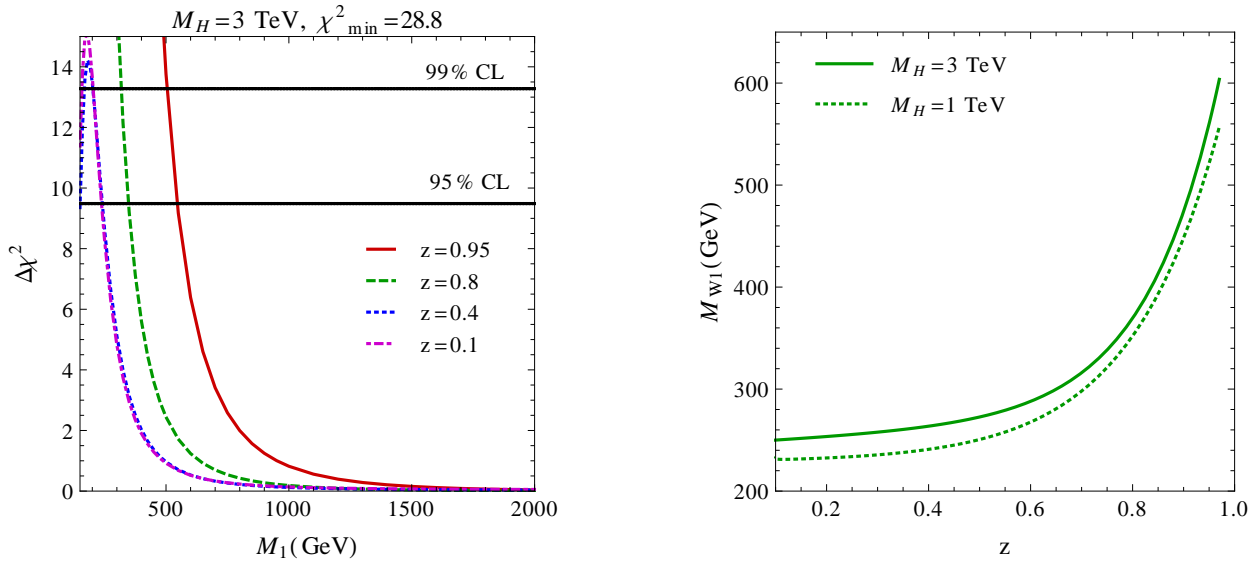


FIG. 3: Left:  $\Delta\chi^2 = \chi^2(z, M_1) - \chi^2_{\min}$  function versus the bare mass parameter  $M_1$ , for four representative values of the free parameter  $z$  (see legend), once fixing the two remaining  $b_{1,2}$  parameters at their optimal values. We choose  $M_H=3$  TeV and use the correlated  $\epsilon_{1,2,3}$  analysis of Eq. (15). The intersecting horizontal lines represent the 95% and 99% CL bound. Right: Minimum mass of the lighter charged gauge boson  $W_1^\pm$  as a function of  $z$ . We fix  $b_{1,2}$  to their optimal values, and consider two values of the  $M_H$  parameter:  $M_H=1$  TeV (dashed line) and  $M_H=3$  TeV (solid line). We take the 95% CL EWPT bound from the left plot.

results are shown in Fig. 4. In the left plot, we display the 95% CL contour plot from the two  $\epsilon_1$  and  $\epsilon_3$  parameters separately, extracting their individual contributions from Eq. (20). There are two main information contained here. First, one can see that while  $\epsilon_3$  forces the two  $b_1, b_2$  couplings to be almost linearly dependent,  $\epsilon_1$  imposes strong constraints on their magnitude. The two  $\epsilon_{1,3}$  parameters play both an important role. Hence, oppositely to what commonly done in the literature where the  $\epsilon_1$  tree level contribution is neglected, it is mandatory to consider them jointly when deriving the physical properties of the extra gauge bosons predicted by Higgsless models. The second information concerns the effect of the  $M_H$  parameter. As clearly shown, it slightly affects only the  $b_1, b_2$  contour coming from the  $\epsilon_1$  parameter. In the right plot of Fig. 4, we show the 95% CL bound on the  $b_1, b_2$  plane coming from the fully correlated  $\epsilon_{1,2,3}$  analysis of Eq. (20). As expected, the correlation shrinks the allowed  $b_1, b_2$  area compared to the naive uncorrelated  $\epsilon_{1,3}$  overlapping strip. Nevertheless, relatively sizable values for the bare direct couplings,  $b_{1,2}$  are allowed by EWPT. These



values are mildly affected by the choice of  $M_H$ . In the following, we fix  $M_H=3$  TeV. The

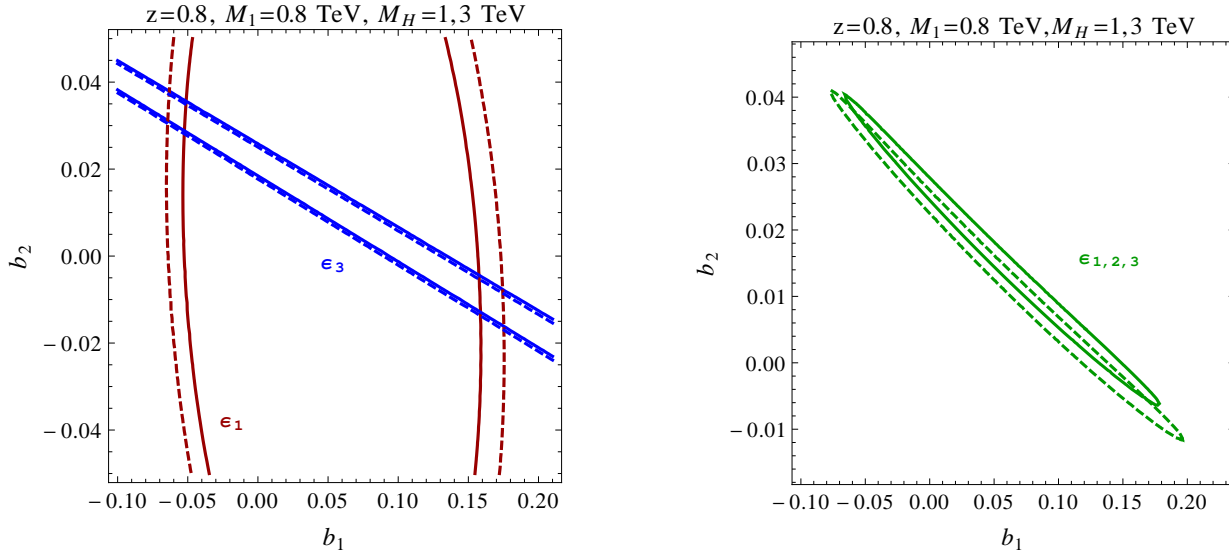


FIG. 4: Left: 95% CL EWPT bounds in the  $b_1, b_2$  plane at fixed  $z=0.8$  and  $M_1=800$  GeV (i.e.  $M_2=1$  TeV) from the individual  $\epsilon_{1,3}$  parameters. The dashed lines correspond to  $M_H=1$  TeV, the solid ones to  $M_H=3$  TeV. Right: 95% CL EWPT bound on the  $b_1, b_2$  plane at fixed  $z=0.8$  from the fully correlated  $\epsilon_{1,2,3}$  analysis.

above mentioned results can be translated into direct limits on the physical couplings of the new vector bosons to SM fermions. In Fig. 5, we focus on the charged gauge sector, and we plot the 95% CL EWPT bounds in the physical mass-coupling plane for the lighter (left plot) and heavier (right plot) extra vector bosons,  $W_{1,2}^\pm$ . We choose four representative values for the  $z$  free parameter:  $z=0.1, 0.4, 0.8$  and  $0.95$ . The mass range is limited by the minimum mass previously discussed, and the upper bound coming from the perturbative unitarity requirement (see Ref. [53, 62, 63] for details). We should also notice that the signs of the physical fermion-boson couplings are completely arbitrary and physically irrelevant (of course the couplings of the different types of fermions to the same neutral boson are not independent though). However, in the  $b_1, b_2$  regions allowed by EWPT, there is an almost two-fold degeneracy in the value of each of the couplings. Two such points in the  $b_1, b_2$  plane, for a given physical coupling, are not exactly equivalent as the other fermion couplings would not generally be the same. Therefore we chose to give different signs to the physical couplings depending on which side of the allowed parameter-space they correspond to. Fig. 5 shows that the  $z$  dependence is quite strong. For high-intermediate  $z$  values,

the allowed portion of the parameter space is large, and accommodates large values of the gauge couplings to SM fermions. With decreasing  $z$ , the gauge boson-fermion couplings get drastically reduced, approaching the almost fermiophobic scenario in the limit where  $z$  tends to zero (in this case of course the heavier gauge boson decouples, and one recover the minimal 3-site Higgsless model with only  $W_1^\pm$  and  $Z_1$ ). For sake of completeness, in

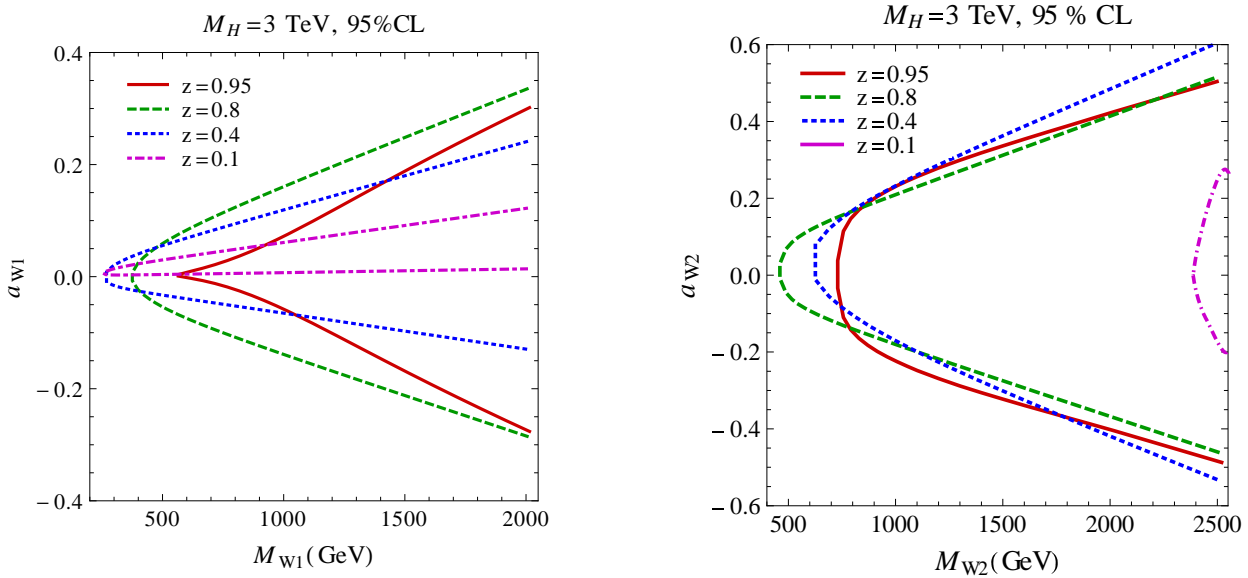


FIG. 5: Left: 95% CL EWPT bound in the parameter space given in terms of physical mass,  $M_{W1}$ , and physical coupling between the lighter extra gauge boson and SM fermions,  $a_{W1}$  (see Eq. A8). We fix  $M_H = 3 \text{ TeV}$ , and consider four different  $z$  values:  $z = 0.1, 0.4, 0.8$  and  $0.95$  (see legend for linestyle code). Right: same for the heavier extra gauge boson  $W_2^\pm$ .

Fig. 6 we show also the 95% CL EWPT bounds in the mass-coupling plane for the neutral gauge sector. We choose as reference the couplings between extra neutral gauge bosons and SM left-handed electrons,  $a_{Z_i} = a_{Z_i}^L(e)$  with  $i = 1, 2$ . We fix  $z = 0.8$ . The left plot (solid line) gives the parameter space for the lighter neutral gauge boson,  $Z_1$ , where this time the gauge coupling is normalized to the corresponding SM one ( $a_Z = a_Z^L(e)$ ). As comparison, the lighter charged gauge boson parameter space is also shown (dashed line). Neutral and charged gauge couplings to ordinary matter are comparable in size. Moreover, they can be of the same order of magnitude than the corresponding SM ones. Analogously, the right plot of Fig. 6 shows that the same is true for the heavier extra gauge boson,  $Z_2$ . In this case, the neutral gauge couplings can be even bigger than the SM ones up to a factor 1.5. Finally, let us notice that the gauge couplings of the heavier resonances are stronger than

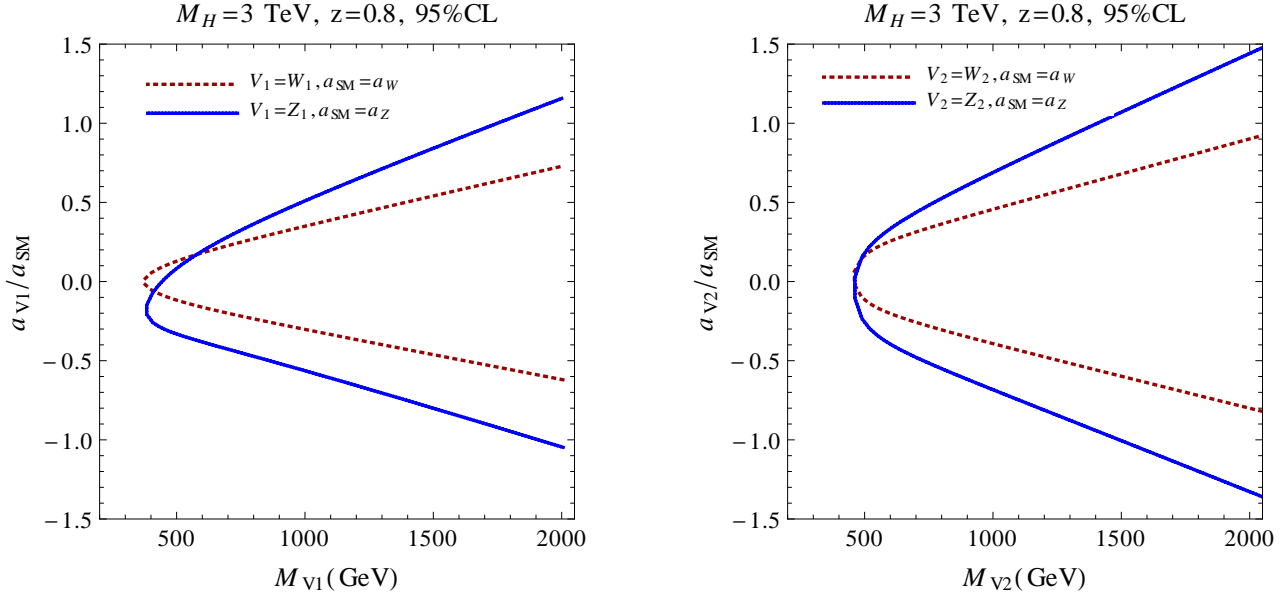


FIG. 6: Left: The solid line represents the 95% CL EWPT bound in the physical mass-coupling plane for the lighter neutral gauge boson  $Z_1$ , at fixed  $z=0.8$ . The mass is denoted by  $M_{Z1}$ . For the coupling, we choose as reference the gauge boson coupling to SM left-handed electrons, normalized to the corresponding SM one,  $a_{Z1}/a_Z$ . As comparison, the dashed line gives the parameter space of the lighter charged gauge boson. Right: same for the heavier resonances  $Z_2$  and  $W_2^\pm$ .

those of the lighter ones. This is a peculiar feature of the 4-site Higgsless model, and can have important phenomenological consequences. If realized in nature, the heavier bosons could indeed produce more events than the lighter ones.

Summarizing, the new exact tree level computation of the EWPT bounds on the 4-site Higgsless model shows that the surviving parameter space is quite large. Oppositely to the minimal 3-site Higgsless model, which is strongly constrained to be almost fermiophobic by EWPT as we will discuss in Sect. VI, its next-to-minimal 4-site extension can accommodate sizeable couplings between extra resonances and SM fermions. The 4-site model, other than better describing the extra dimensional content of Higgsless theories characterized by the presence of multiple resonances, has thus the potential of being detected during the early stage of the LHC experiment in the Drell-Yan channel.

## V. APPROXIMATE VERSUS EXACT SOLUTION

In Refs. [53, 62], we computed the  $\varepsilon_{1,2,3}$  parameters via a perturbative expansion in  $x = e/g_1$ , where  $e$  is the electric charge and  $g_1$  the extra gauge coupling. We calculated all terms up to the second order,  $\mathcal{O}(x^2)$ , keeping the full content in the two direct gauge boson-fermion couplings or delocalization parameters,  $b_{1,2}$ . For completeness, key steps of the procedure and approximate expressions for the  $\varepsilon_{1,2,3}$  parameters are summarized in Appendix A. In order to analyze the validity domain of the  $\mathcal{O}(e^2/g_1^2)$  approximation, in

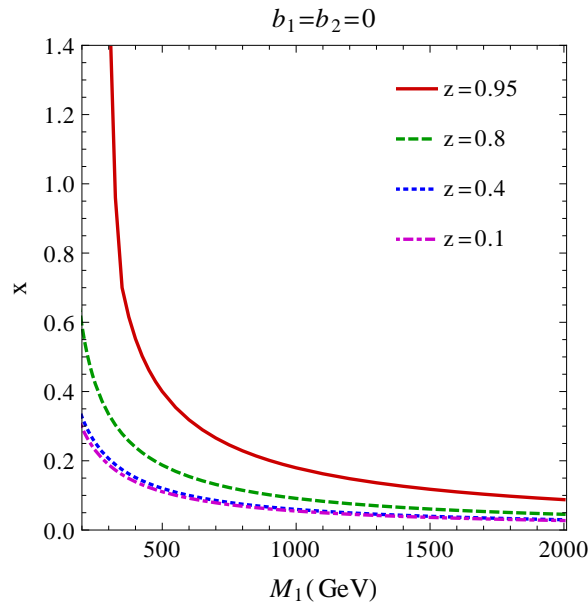


FIG. 7: Expansion parameter,  $x = e/g_1$ , as a function of the bare mass,  $M_1$ , for  $z=0.1, 0.4, 0.8$ , and  $0.95$ . We fix  $b_{1,2} = 0$ .

Fig. 7 we plot the expansion parameter  $x$  as a function of the bare mass  $M_1$  for four values of the free  $z$  parameter:  $z=0.1, 0.4, 0.8$ , and  $0.95$ . While at large masses ( $M_1 \gtrsim 1$  TeV) the neglected higher order terms are expected not to exceed the permil level, they become more and more important with decreasing  $M_1$ . Also, they are not negligible approaching the limit  $z \rightarrow 1$ . This qualitatively indicates that, the series expansion breaks down for low masses ( $M_1 \lesssim 1$  TeV) and high  $z$  values ( $z \sim 1$ ). In order to explore these regions, using the exact numerical calculation of the  $\varepsilon_i$  parameters is mandatory. More quantitatively, in Fig. 8 we compare approximate and exact 95% CL EWPT bounds in the  $b_1, b_2$  plane for  $z=0.8$  and  $M_1=400$  GeV. In the left plot, we consider the individual  $\varepsilon_1$  and  $\varepsilon_3$  contributions to Eq. (20) separately. And for each  $\varepsilon_i$  ( $i=1,3$ ) we show two progressive computational steps:

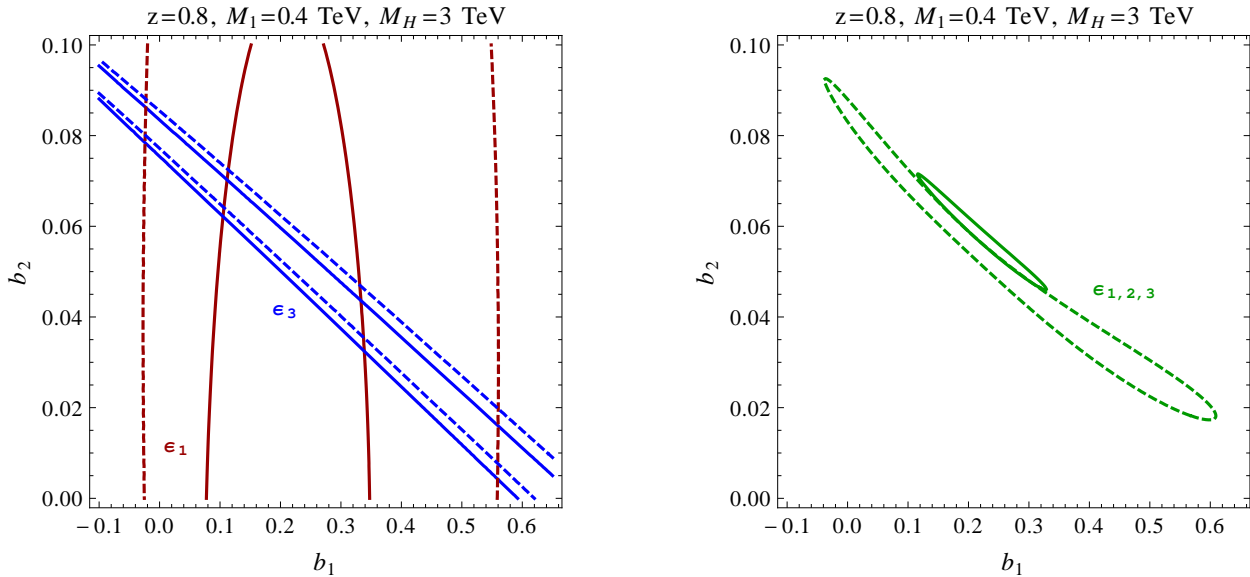


FIG. 8: Left: Comparison between exact (solid line) and  $\mathcal{O}(x^2)$  approximate (dashed line) 95% CL EWPT bound on the  $b_1, b_2$  plane for  $z=0.8$  and  $M_1=0.4$  TeV. We use the individual  $\varepsilon_1$  and  $\varepsilon_3$  contributions to Eq. ((20)). Right: Same, but employing the full correlated  $\varepsilon_{1,2,3}$  analysis.

the approximate results which take into account terms up to  $\mathcal{O}(x^2)$  including the complete  $b_{1,2}$  content (dashed curves), and the exact numerical calculation at all orders (solid curves). The parameter  $\varepsilon_2$  doesn't give any contribution in the range shown. We see that the  $\mathcal{O}(x^2)$  result is in good agreement with the exact result for  $\varepsilon_3$ , while it fails in describing  $\varepsilon_1$ . In the latter case, the exact contour drastically differs from the  $\mathcal{O}(x^2)$  approximate one. As a reference, in Appendix A, the  $\mathcal{O}(x^2)$  expressions for the  $\varepsilon_{1,2,3}$  parameters are reported. These cumbersome formulas are exact in  $b_{1,2}$ . They would assume a much simpler form by performing either a first or even a second-order expansion in the  $b_{1,2}$  parameters as well. This further approximations are largely used in the literature. However our finding is that some cancelations may occur and there is very little control over the validity of the expansion (in particular one shouldn't neglect  $x^2 b_{1,2}$  terms), so we did not expand in  $b_{1,2}$  at all. In the right plot of Fig. 8, we display the exact (solid line) and  $\mathcal{O}(x^2)$  approximate (dashed line) 95% CL EWPT bound on the  $b_1, b_2$  plane for  $z=0.8$  and  $M_1=400$  GeV, taking into account the correlated  $\varepsilon_{1,2,3}$  analysis. The difference between the two calculations is certainly remarkable.

To analyze the consequences of this behavior on the physical quantities, in Fig. 9 we plot exact (solid line) and  $\mathcal{O}(x^2)$  truncated (dashed line) 95% CL EWPT bounds in the mass-

coupling plane. We select the parameter space  $(M_{W_1}, a_{W_1})$  of the lighter charged gauge boson. The figure confirms that for low masses,  $M_1 \lesssim 1$  TeV, the approximation is not reliable anymore.

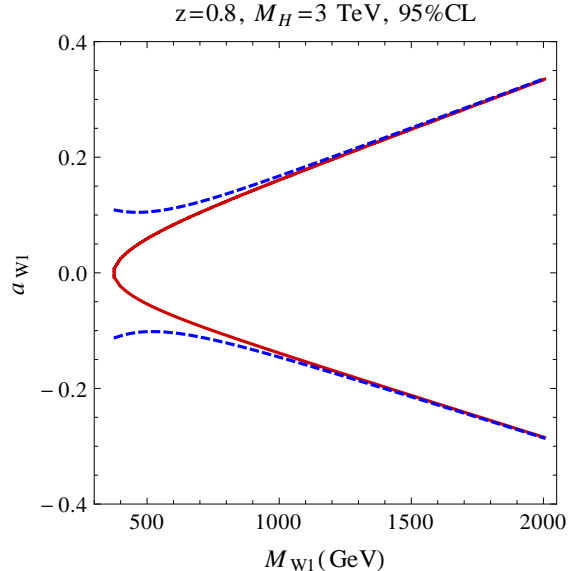


FIG. 9: Comparison of the allowed region at 95% CL in the plane  $(M_{W_1}, a_{W_1})$  between the approximated (blue dashed) and exact (red solid) solution for  $z = 0.8$ .

## VI. 3-SITE HIGGSLESS MODEL AND EWPT BOUNDS

In this section, we specialize our results to the so called 3-site Higgsless model. This model can be seen either as the minimal  $K = 1$  case of deconstructed theories [45], or as the BESS model with  $\alpha = 1$  [47]. By imposing the LR symmetry in the gauge sector, it is a priori described by five parameters  $(\tilde{g}, \tilde{g}', g_1, f_1, b_1)$ . Fixing the gauge parameters  $\tilde{g}, \tilde{g}', g_1$  in terms of the three SM inputs  $e, G_F, M_Z$  as done before for the 4-site model, the number of independent model parameters gets reduced to two:  $M_1$  and  $b_1$ . These are the bare mass and the direct couplings to SM fermions of the new gauge boson triplet, respectively. The 3-site model can be obtained from its 4-site extension by taking the limit  $M_2 \rightarrow \infty$  and  $b_2 = 0$  with  $M_1$  finite (or  $z = b_2 = 0$  with  $M_1$  finite).

Analogously to what done for the 4-site model, we now derive the EWPT bounds on the 3-site Higgsless model, using an exact numerical algorithm. Since we have only two free parameters,  $M_1, b_1$ , the previous Eq. (20) must be replaced by

$$\Delta\chi^2 = \chi^2 - \chi_{min}^2 \leq 5.99(9.21) \quad (21)$$

where the value 5.99(9.21) corresponds to a 95(99)% CL for a  $\chi^2$  with two degrees of freedom. As we can see from Fig. 3, the  $\chi_{min}^2$  value is almost independent on  $z$  and  $M_1$  (for  $M_1 \gtrsim 1\text{TeV}$ ). Thus, its value within the 3-site model is not expected to differ from that one we have in the 4-site model. We indeed obtain  $\chi_{min}^2=28.8$  for  $M_H=3\text{ TeV}$ . By applying Eq. (21), we derive the 95% CL EWPT bound on the  $(M_1, b_1)$  plane, as shown in the left plot of Fig. 10. The wider region represents the bound coming from the individual  $\varepsilon_1$  contribution to Eq. (21). The narrow internal area shows instead the analogous bound from  $\varepsilon_3$ . In this case, the EWPT constraints on the model are completely dominated by the  $\varepsilon_3$  parameter. The fully correlated EWPT bound is the gray region and it is quite near to the one from  $\varepsilon_3$ . These results are obtained via an exact numerical computation. Let us notice however that, within the 3-site Higgsless model, the approximate double expansion in the  $x = e/g_1$  and  $b_1$  parameters works quite well. The following analytical expressions for the  $\varepsilon_{1,3}$  parameters

$$\varepsilon_1 \simeq -\frac{b_1^2}{4}, \quad \varepsilon_3 \simeq \frac{1}{2}(x^2 - b_1) \quad (22)$$

are in excellent agreement with the exact result. Within the minimal 3-site model, one can thus safely apply a series expansion at second order in  $x$  and first order in the delocalization parameter  $b_1$ , neglecting the  $\varepsilon_1$  contribution to the EWPT bounds.

The bounds on the two free parameters of the model can be translated into the physical plane. In the right plot of Fig. 10, we show the EWPT constraint in the mass-coupling plane  $(M_{W1}, a_{W1})$ . Here,  $M_{W1}$  denotes the physical mass of the charged extra gauge boson, while  $a_{W1}$  represents its coupling to SM fermions. We clearly see that the allowed region is quite tiny, and the couplings are very small. Compared to the 4-site model, while in the limit  $z \rightarrow 0$  the 3-site model is recovered, couplings about five times larger can be allowed for larger values of  $z$ . This feature has important phenomenological consequences. In their minimal representation (or 3-site), deconstructed theories appear to be observable only in production channels driven by triple and quartic gauge boson self couplings, the minimal scenario almost fermiophobic. For that reason, the Higgsless literature is mostly focused on difficult multi-particle processes like vector boson fusion and associated production of new gauge bosons with SM ones [58–60]. This is however the result of a crude theoretical approximation. Deconstructed theories can express their extra dimensional nature and their physical properties in a more complete and realistic way via their next-to-minimal 4-site representation. This  $K = 2$  moose model, even if truncated, gives in fact the first

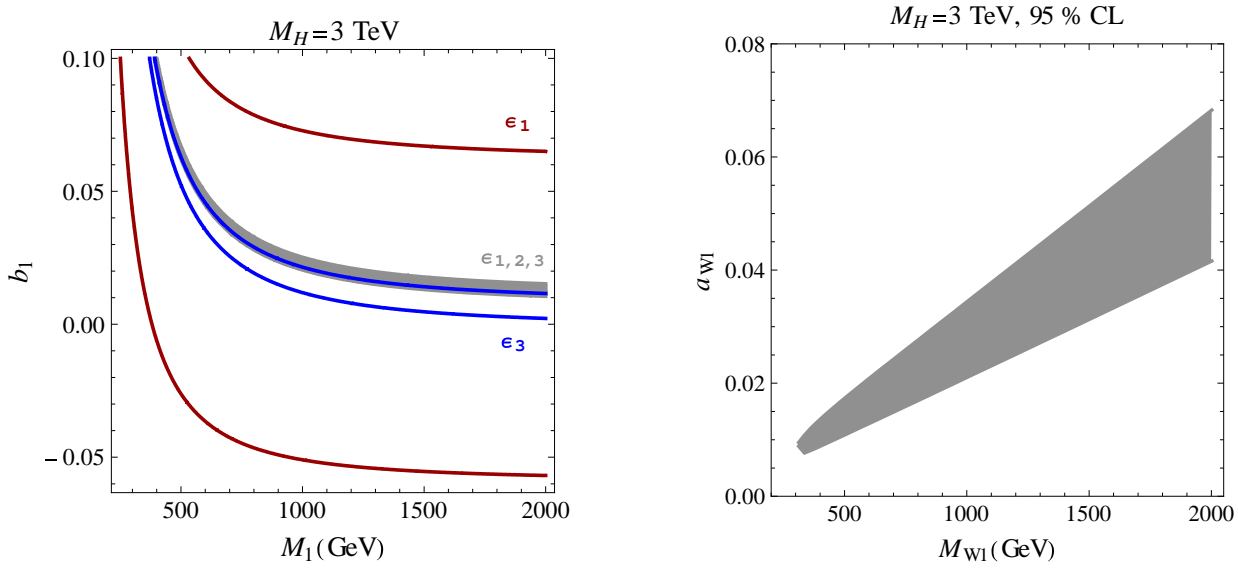


FIG. 10: Left: 95% CL EWPT bound in the bare parameter plane  $(M_1, b_1)$ . The wider region corresponds to the individual  $\epsilon_1$  contribution to Eq. (21), the internal narrow region to the analogous  $\epsilon_3$  contribution. The fully correlated EWPT bound is given by the gray region. Right: 95% EWPT bound in the physical mass-coupling plane  $(M_{W1}, a_{W1})$  from the fully correlated  $\epsilon_{1,2,3}$  analysis. We fix  $M_H = 3 \text{ TeV}$ .

representation of the multi-resonance nature of extra dimensional theories characterized by KK excitation towers. The addition of one more site, to the 3-site, changes completely the physical properties of the predicted extra gauge bosons. The 4-site scenario is not fermiophobic anymore. It thus allows to search for evidence also in production processes driven by boson-fermion couplings. In particular, within the 4-site model, the new resonances could be observed in the favoured Drell-Yan channel already with the data collected in the early stage of the LHC experiment. A first phenomenological analysis of the 4-site model at the LHC is given in [53, 62, 63]

## VII. CONCLUSIONS

In this paper, we have derived the EWPT bounds on the 4-site Higgsless model, which appears as the next-to-minimal deconstructed  $SU(2)$  theory in five dimensions [1, 3–11, 26]. The model is based on the  $SU(2)_L \times SU(2)_1 \times SU(2)_2 \times U(1)_Y$  gauge symmetry, and predicts four charged  $W_{1,2}^\pm$  and two neutral  $Z_{1,2}$  extra gauge bosons. Its novelty, compared



to the minimal 3-site representation, consists in reconciling EWPT bounds and unitarity constraints without imposing the extra vector bosons to be fermiophobic (owing to the inclusion of direct fermion-boson gauge couplings in addition to those ones coming from usual mixing terms).

The phenomenology of the 4-site Higgsless model is controlled by only four free parameters beyond the SM ones: the bare masses,  $M_{1,2}$ , of lighter and heavier extra gauge boson triplets and their bare direct couplings to SM fermions,  $b_{1,2}$ . In this paper, we have performed a new analysis of the EWPT constraints on the aforementioned 4-dimensional parameter space. We used the  $\varepsilon_{1,2,3}$  parametrization of the universal electroweak radiative corrections to the precision observables measured by LEP, SLD and TEVATRON experiments. We neglected the  $\varepsilon_b$  effect, as it is weakly correlated to the other measurements and also because it receives no contribution within the 4-site model owing to universality in the fermionic sector.

The four main novelties of our analysis can be summarized as follows. We computed for the first time the  $\varepsilon_i$  ( $i=1,2,3$ ) parameters at tree level via a complete numerical algorithm, going beyond commonly used analytical approximations. In addition, we have taken into account the full correlation between their measurements, performing a well defined and complete statistical analysis, based on the minimum  $\chi^2$  test. We furthermore studied the cutoff dependence of the derived EWPT bounds, and discussed how well the 4-site Higgsless model can reproduce experimental results. We have finally shown a one-to-one comparison between the EWPT surviving parameter space, given in terms of physical mass and coupling of the first charged resonance ( $M_{W1}, a_{W1}$ ), within the minimal (3-site) and next-to-minimal (4-site) deconstructed Higgsless models.

Our findings are as follows. The popular approximations existing in the literature cannot give a reliable description of masses and couplings allowed by EWPT over the full parameter space. The second-order expansion in the  $x = e/g_1$  parameter, keeping the full dependence on the direct gauge boson-fermion couplings  $b_{1,2}$  as reported in Appendix A, is indeed valid only beyond  $\mathcal{O}(\text{TeV})$  mass scales and for low-intermediate values of the ratio  $z = M_1/M_2$  between the bare masses of the two predicted gauge triplets ( $z \lesssim 0.8$ ). The validity range is mainly constrained by the  $\varepsilon_1$  parameter,  $\varepsilon_3$  being rather stable under the series expansion in  $x$ . Further truncating this  $\mathcal{O}(x^2)$  expansion up to either first-order or even second-order terms in the remaining  $b_{1,2}$  parameters as well, as commonly done in the literature, would worsen the goodness of the approximation sensibly. Taking into account the complete

contribution from the delocalization parameters,  $b_{1,2}$ , is thus mandatory in order to extract reliable EWPT bounds on the 4-site model. This also implies that one should consider  $\varepsilon_1$  on the same footing as  $\varepsilon_3$ . Despite the fact that at leading order in the three parameters  $x, b_1, b_2$ , they go like  $\varepsilon_1 \simeq b_i^2$  and  $\varepsilon_3 \simeq b_i + x^2$ , both  $\varepsilon_{1,3}$  play a strong role. The  $\varepsilon_3$  parameter generates an almost linear relation between the gauge couplings of lighter and heavier extra resonances with ordinary matter, while  $\varepsilon_1$  constrains their size.

The new complete calculation of the EWPT bounds presented in this paper takes into account all  $\varepsilon_i$  ( $i=1,2,3$ ) parameters with their full correlation. We have found that this has indeed a significant effect in extracting the allowed parameter space, as compared to previously used simple analysis. The cutoff dependence of our results is instead rather mild. Its major effect appears in the minimum  $\chi^2$  value that one can obtain within the 4-site model. This value rapidly increases with the cutoff.

All these combined effects determine the portion of the parameter space which survives to EWPT. The four-dimensional parameter space of the 4-site model can be expressed in terms of physical masses and couplings to fermions of the extra gauge bosons. A first EWPT effect is to put a lower bound on the mass spectrum. If we take the lighter charged extra gauge boson  $W_1^\pm$  as representative, we find indeed that its minimum mass can range between  $M_{W_1}^{min}=250$  and 600 GeV for  $0.1 < z < 0.95$ . The second important result is that, even if bounded, the gauge couplings of the six extra gauge bosons to ordinary matter can be of the same order of magnitude than the corresponding SM ones. This is in contrast with the almost fermiophobic scenario of the minimal 3-site representation of Higgsless theories. The addition of one more site brings a drastic change. The next-to-minimal 4-site extension can in fact express the multi-resonance nature of extra-dimensional theories, characterized by Kaluza-Klein excitation towers, and give a less constrained description of the physical properties of the predicted extra gauge bosons.

An immediate phenomenological consequence is that the Drell-Yan production process becomes an open channel for the direct search of these new resonances already during the present data collection by LHC and TEVATRON experiments. A first phenomenological analysis of the 4-site model was done in Ref. [62] and refined in Ref. [63] with a focus on the neutral gauge sector  $Z_{1,2}$ . A detailed study concerning exclusion at the TEVATRON and discovery reach at the LHC is now under investigation.

### Acknowledgments

E.A. and D.B. acknowledge financial support from the NExT Institute and SEPnet. The work of S.D.C., D.D. and L.F. is partly supported by the Italian Ministero dell'Istruzione, dell'Università e della Ricerca Scientifica, under the COFIN program (PRIN 2008).

### Appendix A: Approximated analytical expressions for $\epsilon_1, \epsilon_2, \epsilon_3$

We collect here some analytical formulas, which are necessary to express the predictions for the observables of the 4-site model in terms of physical quantities and the new parameters. All the following definitions are expressed in terms of the model parameters  $g_1, \tilde{g}, \tilde{g}', M_1, z = M_1/M_2, b_1, b_2$ . Let us start with the mass eigenvalues. At the order  $(\tilde{g}/g_1)^2$  they are:

$$M_W^2 = \tilde{M}_W^2 (1 - \tilde{x}^2 z_W), \quad M_Z^2 = \tilde{M}_Z^2 (1 - \tilde{x}^2 z_Z) \quad (\text{A1})$$

$$M_{W_1}^2 = M_1^2 \left(1 + \frac{\tilde{x}^2}{2}\right), \quad M_{W_2}^2 = \frac{M_1^2}{z^2} \left(1 + \frac{\tilde{x}^2 z^4}{2}\right) \quad (\text{A2})$$

$$M_{Z_1}^2 = M_1^2 \left(1 + \frac{\tilde{x}^2}{2\tilde{c}^2}\right), \quad M_{Z_2}^2 = \frac{M_1^2}{z^2} \left(1 + \frac{\tilde{x}^2 z^4}{2\tilde{c}^2}\right) \quad (\text{A3})$$

with

$$\tilde{M}_W^2 = \frac{\tilde{x}^2}{2}(1 - z^2)M_1^2, \quad \tilde{M}_Z^2 = \frac{\tilde{M}_W^2}{\tilde{c}^2}, \quad \tilde{x} = \frac{\tilde{g}}{g_1} \quad (\text{A4})$$

$$z_W = \frac{1}{2}(1 + z^4), \quad z_Z = -2\tilde{s}^2 + \frac{z_W}{\tilde{c}^2} \quad (\text{A5})$$

and  $\tan \tilde{\theta} \equiv \tilde{s}/\tilde{c} = \tilde{g}'/\tilde{g}$ . We recall also the couplings of  $A^\mu, Z^\mu, Z_{1,2}^\mu, W^\mu, W_{1,2}^\mu$ , to fermions:

$$\begin{aligned} \mathcal{L}_{NC} &= \bar{\psi} \gamma^\mu \left[ -e \mathbf{Q}^f A_\mu + a_Z^f Z_\mu + a_{Z_1}^f Z_{1\mu} + a_{Z_2}^f Z_{2\mu} \right] \psi \\ \mathcal{L}_{CC} &= \bar{\psi} \gamma^\mu T^- \psi \left( a_W W_\mu^+ + a_{W_1} W_{1\mu}^+ + a_{W_2} W_{2\mu}^+ \right) + h.c. \end{aligned} \quad (\text{A6})$$

where:

$$\begin{aligned} e &= \tilde{g}\tilde{s} (1 - \tilde{x}^2 \tilde{s}^2) \\ a_Z^f &= -\frac{\tilde{g}}{\tilde{c}} \left(1 - \frac{b}{2}\right) \left(1 + \tilde{x}^2 \left(-\frac{z_Z}{2} + z_{Zb}\right)\right) \left[ \mathbf{T}_3^f - \tilde{s}^2 \frac{1 + \tilde{x}^2(\tilde{c}^2 - \tilde{s}^2 - z_{Zb})}{(1 - \frac{b}{2})} \mathbf{Q}^f \right] \\ a_{Z_1}^f &= -\frac{g_1}{\sqrt{2}(1 + b_+)} \left(b_+ - \frac{\tilde{x}^2}{\tilde{c}^2}(1 + z_1^n)\right) \mathbf{T}_3^f + \frac{g_1 \tilde{x}^2 \tilde{s}^2}{\sqrt{2} \tilde{c}^2} \mathbf{Q}^f \\ a_{Z_2}^f &= -\frac{g_1}{\sqrt{2}(1 + b_+)} \left(b_- - \frac{\tilde{x}^2 z^2}{\tilde{c}^2}(1 + z_2^n)\right) \mathbf{T}_3^f - \frac{g_1 \tilde{x}^2 z^2 \tilde{s}^2}{\sqrt{2} \tilde{c}^2} \mathbf{Q}^f \end{aligned} \quad (\text{A7})$$

and

$$\begin{aligned}
a_W &= -\frac{\tilde{g}}{\sqrt{2}} \left(1 - \frac{b}{2}\right) \left(1 + \tilde{x}^2 \left(-\frac{z_W}{2} + z_{Wb}\right)\right) \\
a_{W_1} &= -\frac{g_1}{2(1+b_+)} (b_+ - \tilde{x}^2(1+z_1)) \\
a_{W_2} &= -\frac{g_1}{2(1+b_+)} (b_- - \tilde{x}^2 z^2(1+z_2))
\end{aligned} \tag{A8}$$

with  $z_Z$  and  $z_W$  given in (A5), and

$$z_{Zb} = (1 - z^2) \frac{b_+(\tilde{c}^2 - \tilde{s}^2) + b_- z^4}{2(2 + b_+ + b_- z^2) \tilde{c}^2}, \quad z_{Wb} = (1 - z^2) \frac{b_+ + b_- z^4}{2(2 + b_+ + b_- z^2)} \tag{A9}$$

$$z_1 = \frac{b_+}{4} + b_- \frac{z^2}{2(1 - z^2)}, \quad z_2 = z^2 \left( \frac{b_-}{4} - b_+ \frac{1}{2(1 - z^2)} \right) \tag{A10}$$

$$z_1^n = \frac{b_+(1 - 4\tilde{s}^2)}{4} + b_- \frac{z^2(\tilde{c}^2 - \tilde{s}^2)}{2(1 - z^2)}, \quad z_2^n = \frac{b_- z^2}{4} - b_+ \frac{z^2 - 2\tilde{s}^2}{2(1 - z^2)} \tag{A11}$$

$$b = \frac{b_+ - b_- z^2}{1 + b_+} \quad b_{\pm} = b_1 \pm b_2 \tag{A12}$$

Now we want to write all in terms of  $e, M_Z, G_F$  and the 4-site parameters  $z, b_1, b_2, M_1$  (at the order  $\tilde{x}^2 = (\tilde{g}/g_1)^2$ ). Let us start with  $\tilde{g}$

$$\tilde{g} = \frac{e}{\tilde{s}} (1 + x^2) \Rightarrow \tilde{x} = \frac{x}{\tilde{s}} (1 + x^2), \quad x = \frac{e}{g_1} \tag{A13}$$

By computing the Fermi constant  $G_F$  as:

$$\frac{G_F}{\sqrt{2}} = \frac{a_W^2}{4M_W^2} + \frac{a_{W_1}^2}{4M_{W_1}^2} + \frac{a_{W_2}^2}{4M_{W_2}^2} \tag{A14}$$

we get:

$$\begin{aligned}
\frac{G_F}{\sqrt{2}} &= \frac{e^2}{8M_Z^2 \tilde{c}^2 \tilde{s}^2} \left[ \left(1 - \frac{b}{2}\right)^2 + (1 - z^2) \frac{b_+^2 + z^2 b_-^2}{4(1 + b_+)^2} \right] \\
&+ \frac{e^2 x^2}{8M_Z^2 \tilde{c}^2 \tilde{s}^2} \left[ \left(1 - \frac{b}{2}\right)^2 \left(2 - \frac{z_Z}{\tilde{s}^2} + 2 \frac{z_{Wb}}{\tilde{s}^2}\right) + \left(2 - \frac{z_Z}{\tilde{s}^2}\right) (1 - z^2) \frac{b_+^2 + z^2 b_-^2}{4(1 + b_+)^2} \right] \\
&- \frac{e^2 x^2}{8M_Z^2 \tilde{c}^2 \tilde{s}^2} \frac{1 - z^2}{\tilde{s}^2} \left[ \frac{b_+^2 + z^6 b_-^2}{8(1 + b_+)^2} + \frac{b_+(1 + z_1) + z^4 b_-(1 + z_2)}{2(1 + b_+)^2} \right]
\end{aligned} \tag{A15}$$

Let us now define the Weinberg angle  $\theta$  by [56]:

$$\frac{G_F}{\sqrt{2}} = \frac{e^2}{8s_\theta^2 c_\theta^2 M_Z^2} \tag{A16}$$

with  $s_\theta = \sin \theta$ . So Eq. (A15) and Eq. (A16) imply:

$$\begin{aligned} \frac{e^2}{8s_\theta^2 c_\theta^2 M_Z^2} &= \frac{e^2}{8\tilde{s}^2 \tilde{c}^2 M_Z^2} X + \frac{e^2}{8M_Z^2} x^2 A \quad \Rightarrow \\ \tilde{s}^2 \tilde{c}^2 &= c_\theta^2 s_\theta^2 X (1 + s_\theta^2 c_\theta^2 x^2 A) \end{aligned} \quad (\text{A17})$$

with

$$X = \left(1 - \frac{b}{2}\right)^2 + \frac{\beta}{4} \quad \beta = (1 - z^2) \frac{b_+^2 + z^2 b_-^2}{(1 + b_+)^2} \quad (\text{A18})$$

$$\begin{aligned} A &= \frac{1}{\tilde{s}^2 \tilde{c}^2} \left[ X \left(2 - \frac{z_Z}{\tilde{s}^2}\right) + \left(1 - \frac{b}{2}\right)^2 \frac{2z_{Wb}}{\tilde{s}^2} - \frac{B}{\tilde{s}^2} \right] \\ B &= \frac{1 - z^2}{8(1 + b_+)^2} [b_+^2 + z^6 b_-^2 + 4b_+(1 + z_1) + 4b_- z^4(1 + z_2)] \end{aligned} \quad (\text{A19})$$

Now we can solve this equation perturbatively in  $x$ ; at the  $x^2$  order we get:

$$\tilde{s}^2 = s_*^2 + x^2 \frac{s_\theta^4 c_\theta^4}{\sqrt{1 - s_{2\theta}^2 X}} AX \quad (\text{A20})$$

with:

$$\begin{aligned} s_*^2 &= \frac{1}{2} \left(1 - \sqrt{1 - s_{2\theta}^2 X}\right) \\ s_*^2 c_*^2 &= s_\theta^2 c_\theta^2 X \end{aligned} \quad (\text{A21})$$

with  $\tilde{s}$  and  $\tilde{c}$  replaced by  $s_*$  and  $c_*$  in  $A$  since it is multiplied by  $x^2$ . Namely, by using the zero order of Eq. (A21), we can rewrite the zero order expression for  $A$  as:

$$\begin{aligned} A|_{x=0} &= \frac{1}{s_*^2 c_*^2} \left[ X \left(2 - \frac{z_Z}{s_*^2}\right) + \left(1 - \frac{b}{2}\right)^2 \frac{2z_{Wb}}{s_*^2} - \frac{B}{s_*^2} \right] \\ &= \frac{1}{s_\theta^2 c_\theta^2} \left[ \left(2 - \frac{z_Z}{s_*^2}\right) + \left(1 - \frac{b}{2}\right)^2 \frac{2z_{Wb}}{X s_*^2} - \frac{B}{X s_*^2} \right] \end{aligned} \quad (\text{A22})$$

Then, from Eqs. (A13) and (A1), we get :

$$\begin{aligned}
g_1^2 &= \frac{e^2(1-z^2)M_1^2}{2\tilde{s}^2\tilde{c}^2M_Z^2} \left(1 + x^2 \left(2 - \frac{z_Z}{\tilde{s}^2}\right)\right) \\
&= \frac{e^2(1-z^2)}{2s_*^2c_*^2M_Z^2} (1 - s_\theta^2c_\theta^2x^2A) \left(1 + x^2 \left(2 - \frac{z_Z}{\tilde{s}^2}\right)\right) \\
&= \frac{e^2(1-z^2)}{2s_\theta^2c_\theta^2XM_Z^2} \left[1 + x^2 \left(-\left(1 - \frac{b}{2}\right)^2 \frac{2z_{Wb}}{Xs_*^2} + \frac{B}{Xs_*^2}\right)\right] \\
\tilde{g} &= \frac{e}{s_*} \left[1 + x^2 \left(1 - \frac{s_\theta^4c_\theta^4}{2s_*^2\sqrt{1-s_{2\theta}^2}X}AX\right)\right] \\
x^2 &= 2s_\theta^2c_\theta^2X \frac{M_Z^2}{M_1^2(1-z^2)}
\end{aligned} \tag{A23}$$

Now that we have expressed all in terms of  $e, \theta, M_Z, z, b_1, b_2, g_1$ , we can rewrite the coupling between the  $Z$ -boson and fermions (from Eq. (A7)) as:

$$a_Z^f = -\frac{e}{s_\theta c_\theta} \left(1 + \frac{\Delta\rho}{2}\right) (\mathbf{T}_3^f - s_{eff}^2 \mathbf{Q}^f) \tag{A24}$$

where

$$1 + \frac{\Delta\rho}{2} = \frac{1}{\sqrt{X}} \left(1 - \frac{b}{2}\right) \left[1 + \frac{x^2}{s_*^2} \left(z_{Zb} - \left(1 - \frac{b}{2}\right)^2 \frac{z_{Wb}}{X} + \frac{B}{2X}\right)\right] \tag{A25}$$

and

$$s_{eff}^2 = \tilde{s}^2 \frac{1}{1 - \frac{b}{2}} [1 + \tilde{x}^2(\tilde{c}^2 - \tilde{s}^2 - z_{Zb})] \tag{A26}$$

Therefore

$$\epsilon_1 = \Delta\rho = -2 + \frac{2}{\sqrt{X}} \left(1 - \frac{b}{2}\right) + \frac{2e^2}{s_*^2g_1^2\sqrt{X}} \left(1 - \frac{b}{2}\right) \left[z_{Zb} - \left(1 - \frac{b}{2}\right)^2 \frac{z_{Wb}}{X} + \frac{B}{2X}\right] \tag{A27}$$

with  $z_Z$  and  $z_{Zb}$  given in Eq. (A5) and (A9) with  $\tilde{s} \rightarrow s^*$  and  $\tilde{c} \rightarrow c^*$ . From the definition:

$$s_{eff}^2 = s_\theta^2(1 + \Delta k) \tag{A28}$$

we get:

$$\Delta k = -1 + \frac{s_*^2}{s_\theta^2} \frac{1}{1 - \frac{b}{2}} \left[1 + \frac{x^2}{s_*^2} \left(\frac{s_\theta^4c_\theta^4}{\sqrt{1-s_{2\theta}^2}X}AX + c_*^2 - s_*^2 - z_{Zb}\right)\right] \tag{A29}$$

Furthermore, from  $M_W/M_Z$  we extract  $\Delta r_W$ :

$$\frac{M_W^2}{M_Z^2} = \tilde{c}^2 [1 + \tilde{x}^2(z_Z - z_W)] = c_\theta^2(1 - \frac{s_\theta^2}{c_{2\theta}}\Delta r_W) \tag{A30}$$

and

$$\Delta r_W = \frac{c_\theta^2 - s_\theta^2}{s_\theta^2} \left\{ 1 - \frac{c_*^2}{c_\theta^2} \left[ 1 + x^2 \left( \frac{z_Z}{s_*^2} - \frac{z_W}{s_*^2} - \frac{s_\theta^4 c_\theta^4}{c_*^2 \sqrt{1 - s_{2\theta}^2} X} A X \right) \right] \right\} \quad (\text{A31})$$

Using Eqs. (A27),(A29),(A31) we derive  $\varepsilon_{2,3}$  by using the relations in [56]:

$$\begin{aligned} \epsilon_2 &= c_\theta^2 \Delta \rho + \frac{s_\theta^2}{c_{2\theta}} \Delta r_W - 2s_\theta^2 \Delta k \\ \epsilon_3 &= c_\theta^2 \Delta \rho + c_{2\theta} \Delta k \end{aligned} \quad (\text{A32})$$

- 
- [1] N. Arkani-Hamed, S. Dimopoulos, and G. R. Dvali, Phys. Lett. **B429**, 263 (1998), hep-ph/9803315.
  - [2] I. Antoniadis, N. Arkani-Hamed, S. Dimopoulos, and G. R. Dvali, Phys. Lett. **B436**, 257 (1998), hep-ph/9804398.
  - [3] L. Randall and R. Sundrum, Phys. Rev. Lett. **83**, 3370 (1999), hep-ph/9905221.
  - [4] C. Csaki, C. Grojean, H. Murayama, L. Pilo, and J. Terning, Phys. Rev. **D69**, 055006 (2004), hep-ph/0305237.
  - [5] K. Agashe, A. Delgado, M. J. May, and R. Sundrum, JHEP **08**, 050 (2003), hep-ph/0308036.
  - [6] C. Csaki, C. Grojean, L. Pilo, and J. Terning, Phys. Rev. Lett. **92**, 101802 (2004), hep-ph/0308038.
  - [7] R. Barbieri, A. Pomarol, and R. Rattazzi, Phys. Lett. **B591**, 141 (2004), hep-ph/0310285.
  - [8] Y. Nomura, JHEP **11**, 050 (2003), hep-ph/0309189.
  - [9] G. Cacciapaglia, C. Csaki, C. Grojean, and J. Terning, Phys. Rev. **D70**, 075014 (2004), hep-ph/0401160.
  - [10] G. Cacciapaglia, C. Csaki, C. Grojean, and J. Terning, Phys. Rev. **D71**, 035015 (2005), hep-ph/0409126.
  - [11] R. Contino, T. Kramer, M. Son, and R. Sundrum, JHEP **05**, 074 (2007), hep-ph/0612180.
  - [12] B. W. Lee, C. Quigg, and H. B. Thacker, Phys. Rev. **D16**, 1519 (1977).
  - [13] R. Sekhar Chivukula, D. A. Dicus, and H.-J. He, Phys. Lett. **B525**, 175 (2002), hep-ph/0111016.
  - [14] T. Ohl and C. Schwinn, Phys.Rev. **D70**, 045019 (2004), hep-ph/0312263.
  - [15] M. Papucci (2004), hep-ph/0408058.

- [16] A. Muck, L. Nilse, A. Pilaftsis, and R. Ruckl, Phys.Rev. **D71**, 066004 (2005), hep-ph/0411258.
- [17] N. Arkani-Hamed, A. G. Cohen, and H. Georgi, Phys. Rev. Lett. **86**, 4757 (2001), hep-th/0104005.
- [18] N. Arkani-Hamed, A. G. Cohen, and H. Georgi, Phys. Lett. **B513**, 232 (2001), hep-ph/0105239.
- [19] C. T. Hill, S. Pokorski, and J. Wang, Phys. Rev. **D64**, 105005 (2001), hep-th/0104035.
- [20] H.-C. Cheng, C. T. Hill, S. Pokorski, and J. Wang, Phys. Rev. **D64**, 065007 (2001), hep-th/0104179.
- [21] H. Abe, T. Kobayashi, N. Maru, and K. Yoshioka, Phys. Rev. **D67**, 045019 (2003), hep-ph/0205344.
- [22] A. Falkowski and H. D. Kim, JHEP **08**, 052 (2002), hep-ph/0208058.
- [23] L. Randall, Y. Shadmi, and N. Weiner, JHEP **01**, 055 (2003), hep-th/0208120.
- [24] D. T. Son and M. A. Stephanov, Phys. Rev. **D69**, 065020 (2004), hep-ph/0304182.
- [25] J. de Blas, A. Falkowski, M. Perez-Victoria, and S. Pokorski, JHEP **08**, 061 (2006), hep-th/0605150.
- [26] G. Cacciapaglia, C. Csaki, C. Grojean, and J. Terning, ECONF **C040802**, FRT004 (2004).
- [27] R. Foadi, S. Gopalakrishna, and C. Schmidt, JHEP **03**, 042 (2004), hep-ph/0312324.
- [28] J. Hirn and J. Stern, Eur. Phys. J. **C34**, 447 (2004), hep-ph/0401032.
- [29] R. Casalbuoni, S. De Curtis, and D. Dominici, Phys. Rev. **D70**, 055010 (2004), hep-ph/0405188.
- [30] R. S. Chivukula, E. H. Simmons, H.-J. He, M. Kurachi, and M. Tanabashi, Phys. Rev. **D70**, 075008 (2004), hep-ph/0406077.
- [31] H. Georgi, Phys. Rev. **D71**, 015016 (2005), hep-ph/0408067.
- [32] R. Casalbuoni, S. De Curtis, D. Dominici, and D. Dolce, JHEP **08**, 053 (2007), arXiv:0705.2510 [hep-ph].
- [33] C. W. B. T. Appelquist, Phys. Rev. **D22** **200** (1980).
- [34] A. C. Longhitano, Phys. Rev. **D22** **1166** (1980).
- [35] A. C. Longhitano, Nucl. Phys. **B188** **118** (1981).
- [36] J. Bagger, S. Dawson, and G. Valencia, Nucl. Phys. **B399**, 364 (1993), hep-ph/9204211.
- [37] M. Perelstein, JHEP **10**, 010 (2004), hep-ph/0408072.
- [38] R. S. Chivukula, E. H. Simmons, S. Matsuzaki, and M. Tanabashi, Phys. Rev. **D75**, 075012



- (2007), hep-ph/0702218.
- [39] R. Sekhar Chivukula, E. H. Simmons, H.-J. He, M. Kurachi, and M. Tanabashi, Phys. Rev. **D71**, 035007 (2005), hep-ph/0410154.
  - [40] R. Sekhar Chivukula et al., Phys. Rev. **D74**, 075011 (2006), hep-ph/0607124.
  - [41] G. Cacciapaglia, C. Csaki, C. Grojean, M. Reece, and J. Terning, Phys. Rev. **D72**, 095018 (2005), hep-ph/0505001.
  - [42] R. Foadi, S. Gopalakrishna, and C. Schmidt, Phys. Lett. **B606**, 157 (2005), hep-ph/0409266.
  - [43] R. Foadi and C. Schmidt, Phys. Rev. **D73**, 075011 (2006), hep-ph/0509071.
  - [44] R. S. Chivukula, E. H. Simmons, H.-J. He, M. Kurachi, and M. Tanabashi, Phys. Rev. **D71**, 115001 (2005), hep-ph/0502162.
  - [45] R. Casalbuoni, S. De Curtis, D. Dolce, and D. Dominici, Phys. Rev. **D71**, 075015 (2005), hep-ph/0502209.
  - [46] R. S. Chivukula, E. H. Simmons, H.-J. He, M. Kurachi, and M. Tanabashi, Phys. Rev. **D72**, 015008 (2005), hep-ph/0504114.
  - [47] R. Casalbuoni, S. De Curtis, D. Dominici, and R. Gatto, Phys. Lett. **B155**, 95 (1985).
  - [48] R. Casalbuoni, S. De Curtis, D. Dominici, and R. Gatto, Nucl. Phys. **B282**, 235 (1987).
  - [49] J. Bagger, V. D. Barger, K.-m. Cheung, J. F. Gunion, T. Han, et al., Phys. Rev. **D49**, 1246 (1994), hep-ph/9306256.
  - [50] R. Casalbuoni, S. De Curtis, and D. Dominici, Phys. Lett. **B403**, 86 (1997), hep-ph/9702357.
  - [51] R. Barbieri, G. Isidori, V. S. Rychkov, and E. Trincherini (2008), 0806.1624.
  - [52] R. Barbieri, A. E. Carcamo Hernandez, G. Corcella, R. Torre, and E. Trincherini, JHEP **03**, 068 (2010), 0911.1942.
  - [53] E. Accomando, S. De Curtis, D. Dominici, and L. Fedeli, Phys. Rev. **D79**, 055020 (2009), 0807.5051.
  - [54] M. E. Peskin and T. Takeuchi, Phys. Rev. Lett. **65**, 964 (1990).
  - [55] M. E. Peskin and T. Takeuchi, Phys. Rev. **D46**, 381 (1992).
  - [56] G. Altarelli and R. Barbieri, Phys. Lett. **B253**, 161 (1991).
  - [57] G. Altarelli, R. Barbieri, and F. Caravaglios, Int. J. Mod. Phys. **A13**, 1031 (1998), hep-ph/9712368.
  - [58] A. Birkedal, K. Matchev, and M. Perelstein, Phys. Rev. Lett. **94**, 191803 (2005), hep-ph/0412278.

- [59] A. Belyaev (2007), 0711.1919.
- [60] H.-J. He et al., Phys. Rev. **D78**, 031701 (2008), 0708.2588.
- [61] T. Ohl and C. Speckner, Phys.Rev. **D78**, 095008 (2008), 0809.0023.
- [62] E. Accomando, S. De Curtis, D. Dominici, and L. Fedeli, Nuovo Cim. **123B**, 809 (2008), 0807.2951.
- [63] E. Accomando, S. De Curtis, D. Dominici, and L. Fedeli, Phys.Rev. **D83**, 015012 (2011), 1010.0171.
- [64] G. Altarelli, R. Barbieri, and F. Caravaglios, Nucl. Phys. **B405**, 3 (1993).
- [65] R. Casalbuoni, S. De Curtis, D. Dominici, F. Feruglio, and R. Gatto, Int. J. Mod. Phys. **A4**, 1065 (1989).
- [66] W. M. Yao et al. (Particle Data Group), J. Phys. **G33**, 1 (2006).
- [67] J. Bechi, R. Casalbuoni, S. De Curtis, and D. Dominici, Phys. Rev. **D74**, 095002 (2006), hep-ph/0607314.
- [68] R. Barbieri, A. Pomarol, R. Rattazzi, and A. Strumia, Nucl. Phys. **B703**, 127 (2004), hep-ph/0405040.
- [69] S. Matsuzaki, R. S. Chivukula, E. H. Simmons, and M. Tanabashi, Phys. Rev. **D75**, 073002 (2007), hep-ph/0607191.
- [70] R. S. Chivukula, E. H. Simmons, S. Matsuzaki, and M. Tanabashi, Phys. Rev. **D75**, 075012 (2007), hep-ph/0702218.
- [71] S. Dawson and C. Jackson, Phys.Rev. **D76**, 015014 (2007), hep-ph/0703299.
- [72] S. Dawson and C. B. Jackson, Phys. Rev. **D79**, 013006 (2009), 0810.5068.
- [73] V. A. Miransky, M. Tanabashi, and K. Yamawaki, Phys. Lett. **B221**, 177 (1989).
- [74] V. A. Miransky, M. Tanabashi, and K. Yamawaki, Mod. Phys. Lett. **A4**, 1043 (1989).
- [75] W. A. Bardeen, C. T. Hill, and M. Lindner, Phys. Rev. **D41**, 1647 (1990).
- [76] C. T. Hill, Phys. Lett. **B345**, 483 (1995), hep-ph/9411426.
- [77] C. T. Hill, Phys. Lett. **B266**, 419 (1991).
- [78] T. Han, D. L. Rainwater, and G. Valencia, Phys. Rev. **D68**, 015003 (2003), hep-ph/0301039.
- [79] ALEPH Collaboration, DELPHI Collaboration, L3 Collaboration, OPAL Collaboration, SLD Collaboration, LEP Electroweak Working Group, SLD Electroweak Group, SLD Heavy Flavour Group, Phys.Rept. **427**, 257 (2006), hep-ex/0509008.
- [80] K. Agashe and R. Contino, Nucl.Phys. **B742**, 59 (2006), hep-ph/0510164.